Antifungal discovery using a microarray-based reporter strategy

Jamie Surprenant

Department of Biochemistry
McGill University
Montreal, Quebec
February, 2008

A thesis submitted to the faculty of Graduate Studies and Research in partial fulfillment of the requirements for the degree of Master of Science.

Abstract

Current treatments for fungal infections involve a small spectrum of drugs, which are becoming ineffective due to the development of resistance among the fungal pathogens. We hypothesized that specific yeast genes are required to maintain viability in the presence of the antifungal fluconazole. By using combination therapy with fluconazole and a yet unidentified compound which targets these genes, this synergistic pair would kill the fungal pathogen. Previous work identified twenty-three genes essential for cell survival in the presence of fluconazole (FCZ-fungicidal). Using microarrays to identify specifically up-regulated genes in the absence of FCZ-fungicidal genes, we set up a growth reporter assay that will signal the inactivation of a FCZ-fungicidal gene or protein. Compounds activating the reporter are potentially synergistic fungicidal with fluconazole. Upon screening a library of known drugs, we identified diphenyleneiodonium chloride as a potential synergistic fungicidal compound with fluconazole, and confirmed the combinatorial fungicidal effectiveness in both *Saccharomyces cerevisiae* and *Candida albicans*.

Résumé

Les traitements actuels contre les infections fongiques n'impliquent qu'un petit éventail de médicaments qui sont susceptibles au développement de résistance parmi les pathogènes fongiques. Notre hypothèse est qu'il existe des gènes de levure essentiels pour maintenir la viabilité des cellules en présence du composé fongistatique fluconazole. En utilisant une thérapie combinatoire avec le fluconazole et un composé qui cible ces gènes, une paire synergique pourrait être développée qui éliminerait les organismes responsables des infections fongiques. Une analyse préliminaire a identifié vingt-trois gènes essentiels pour la survie des cellules en présence du fluconazole (FCZ-fungicidal). En utilisant des micropuces pour identifier des gènes spécifiquement surexprimés dans l'absence des gènes FCZ-fungicidal, nous avons créé une analyse par gène rapporteur qui signal l'inactivation d'un gène FCZ-fungicidal. Des composés activant le reporteur seraient potentiellement synergique fungicidal avec le fluconazole. En criblant une librairie de composés connus, nous avons identifié le chlorure de diphényliodonium comme composé potentiellement synergique fungicidal avec le fluconazole et nous l'avons confirmé chez les souches *Saccharomyces cerevisiae* et *Candida albicans*.

Preface

The work presented herein is essentially my own. The initial screen performed to establish genes essential for cell survival in the presence of fluconazole was performed by Doreen Harcus at the Biotechnology Research Institute (BRI). Further investigation and characterization of these strains was performed by Elaine Tan, Tamiko Nishimura and Dr. Gregor Jansen. The chemical screen was carried out at the McGill high-throughput screening (HTS) facility with Jing Liu and Andy Xiaofeng Wang. The checkerboard synergy assay between fluconazole and diphenyleneiodonium chloride in *Candida albicans* was performed by Elias Epp at the BRI. Anna Y. Lee from the McGill Centre for Bioinformatics (MCB) carried out all the bioinformatics analysis. Dr. Gregor Jansen and Dr. David Y. Thomas provided advice and supervision throughout the course of these studies.

Table of Contents

List of Figures

List of Tables

List of Abbreviations

2YT: 2 Yeast tryptone
3-AT: 3-AminoTriazole
ATCC: American Type Culture Collection
BRI: Biotechnology Research Institute
CFU: Colony Forming Unit
CIVs: Cylindrical IntraVacuolar structure
DEPC: DiEthylPyroCarbonate
DIG: DIGoxigenin
DMSO: DiMethylSulfOxide
DPIC: DiPhenyleneIodonium Chloride
EDTA: EthyleneDiamineTetraAcetic acid
FCZ: FluConaZole
GAL: GALactose
GO: Gene Ontology
GPI: GlycosylPhosphatidylInositol
HAT: Histone AcetylTransferase
HIS: HIStidine
HIV: Human Immunodeficiency Virus
HTS: High-Throughput Screening
ICU: Intensive Care Unit
LEU: LEUcine
LIMMA: LInear Models for MicroArray data
LOPAC: Library of Pharmacologically Active Compounds
MAD: Median Absolute Deviation
MCB: McGill Centre for Bioinformatics
MIC: Minimum Inhibitory Concentration
mTOR: Mammalian Target Of Rapamycin
NCR: Nitrogen Catabolic Repression
OD_{600}: Optical Density value at wavelength 600nm
PCR: Polymerase Chain Reaction
PEG: PolyEthylene Glycol
S.C.: Synthetic Complete
SAB: Sodium Acetate and EDTA Buffer
SAP: Secreted Aspartyl Proteinases
SSC: Sodium chloride and Sodium Citrate
SAGA complex: Spt-Ada-Gcn5-Acetyltransferase complex
SD: Synthetic Drop-out
SDS: Sodium Dodecyl Sulphate
SGA: Synthetic Genetic Array
UHN: University Health Network
URA: URAcil
WT: wild type
YPD: Yeast Peptone Dextrose

Acknowledgements

I would like to acknowledge my supervisor, Dr. David Y. Thomas, for giving me the opportunity to do my Master's degree in his lab, as well as for all his help and support. I would like to thank the numerous people who have been an invaluable source of advice and assistance to me throughout the course of these studies: Dr. Gregor Jansen for his help and advice through every step of the way, Daniel Dignard, at the Biotechnology Research Institute (BRI), for teaching me how to perform microarray analysis, Anna Lee, from the McGill Centre for Bioinformatics, for all the bioinformatics analysis, the McGill HTS facility, more particularly Dr. Jing Liu and Andy Xiaofeng Wang, for helping me with the chemical screens, and finally Elias Epp, at the BRI, for performing the checkerboard synergy assays. Additionally, I would like to express my thanks the members of my Research Advisory Committee, Dr. Malcolm Whiteway and Dr. Mike Hallett, for all their advice. Finally, I would like to express my appreciation to all lab members for their help, advice and especially for making the work atmosphere in the lab such a pleasant experience. I am grateful to my family, friends and Jason for believing in me and supporting me.

Chapter 1

Introduction

1.1 Importance of the search for novel antifungal therapies

Current treatments for fungal infections involve a small spectrum of drugs which have similar modes of action. Some pathogens have already developed resistance to these drugs, meanwhile the number of patients susceptible to fungal infections is growing. Thus, the increasing frequency of drug resistance stemming from the limited number of suitable and effective antifungal drugs in combination with the growing number of patients affected by *Candida* infections emphasizes the necessity of new and better agents that target essential biological processes of fungal species (Naglik, 2003).

1.1.1 *Candida albicans* infections in humans

Candida albicans is the cause of one of the four most common causes of bloodstream infections (Hobson, 2003) and is the single most common fungal species causing nosocomial (hospital-acquired) infections (Haynes, 2001, Voss, 1999). There is a growing risk of acquiring *Candida* infections in hospitals due to the increasing number of patients receiving immunosuppressive anti-neoplastic agents or immunosuppressive transplants. Also, improvements in health care have led to higher survival rates creating a group of long-term intensive care unit (ICU) residents who are at risk of fungal infections.

Candida albicans is a native inhabitant of human skin, the oral cavity, mucosal surfaces and are frequently encountered as part of the human microflora. This pathogenic yeast is so versatile that it is able to survive as a commensal in all of these niches that each have their own specific environmental differences such as diverse pH levels (Calderone, 2001).

Candida albicans expresses virulence factors which contribute to its pathogenesis, these include: adhesin biomolecules, morphogenesis, and secreted aspartyl proteases (Calderone, 2001). Adhesin biomolecules promote the adherence of *C. albicans* to host cells

and proteins resulting in the reduction and perhaps even the prevention of the host from clearing the pathogen.

Morphogenesis refers to *C. albicans*' ability to switch between the two distinct forms: yeast and filamentous. The yeast form is characterized by oval cells that reproduce by budding to form another independent daughter cell. The filamentous form grows by apical extension leading to the appearance of long, thin filaments. There can be branching from these filaments which are referred to as hyphae. Pseudohyphae are chains of yeast-phase cells formed when the mother and daughter cell do not separate. *Candida albicans* is thus considered a polymorphic fungus because yeast, hyphae, and pseudohyphae forms can all be present during infection. It is presumed that there is a relation between morphogenesis and virulence because one morphological form predominates during commensalism and another during the disease process. However, *C. albicans* infections often have all the various different morphologies present and it has been suggested that all forms may be required to maintain the infection (Rooney, 2002).

Proteolytic enzymes, more specifically secreted aspartyl proteinases (Sap), are commonly associated with *C. albicans* virulence. An increase in the level of Sap results in an increase in virulence. The involvement of Sap in *C. albicans* virulence is complex because its production is associated with hyphae formation, adhesion, and phenotypic switching (Naglik, 2003). Although there has been a large amount of research on Saps, there still remain many unanswered questions such as the environmental stimuli that influence *SAP* expression *in vivo*, the signal transduction pathways that regulate the proteinase expression, and the actual targets of the Sap family during infection (Naglik, 2003).

Candida albicans is an opportunistic pathogen and can respond rapidly to environmental changes. Thus, if it encounters host dysfunction generated by such agents as the administration of broad-spectrum antibiotics, neutropenia (abnormal decrease in the

number of neutrophils in blood), or disruption of protective barriers (including catheterisation), it will take advantage of the impaired immunity of the host and cause disease (Haynes, 2001). By administering broad spectrum antibiotics, the normal bacterial flora in the gastrointestinal tract is suppressed, allowing for the yeast to proliferate. For healthy patients this may not produce a systemic infection, however, it may cause life-threatening illness for the critically ill (Vincent, 1998). This colonization precedes candidemia and is most probably a prerequisite for invasive infection (Voss, 1999). Candidemia is defined as the isolation of any pathogenic species of *Candida* from at least one blood culture specimen (Vincent, 1998). Most *Candida albicans* systemic infections are caused by endogenous organisms that in some way translocate from the gastrointestinal tract to other body sites (Vincent, 1998).

The term "disseminated candidiasis" refers to *Candida* infection in multiple non-contiguous organs and implies hematogenous spread of the pathogen. Disseminated candidiasis, involving the formation of micro-abscesses in multiple tissues and organs, is a difficult infection to eradicate, even in the immunocompetent host (Vincent, 1998). Chronic disseminated candidiasis is thought to develop from neutropenia and mucosal damage of the gastrointestinal tract, which can allow colonized *Candida albicans* to infect the host (Choi, 2003). Therapy is aimed at resolving candidemia before disseminated infection can be established.

A second class of infection that can develop from *Candida albicans* is superficial candidiasis. Patients with superficial candidiasis rarely develop invasive candidiasis of parenchymal organs (described above). Superficial candidiasis tends to be quite specific and self-limited in non-immunocompromised hosts. The remedy for these infections involves local treatment and basic hygiene measures. The immunologic basis for the disease is abnormal T lymphocyte function related to the deficient production of cytokines (Kirkpatrick, 2001).

1.1.2 Epidemiology

Patients with suppressed immune systems such as individuals with AIDS, people undergoing tissue transplants and/or various cancer treatments, are particularly susceptible to systemic *Candida* infections (Eggimann, 2003). The rising incidence of human immunodeficiency virus (HIV) infections and the increase of immunosuppressive drug usage for the treatment of autoimmune disorders are fuelling the immediate need to control fungal morbidity and to address the prevention of fungal-induced complications and mortality (Groll, 2002). As mentioned previously, the majority of such systemic infections are caused by *Candida albicans*, and within this patient population mortality can approach 30%, even with correct therapy (Vincent, 1998).

Candida albicans is a common nosocomial infection 70% of all women experience *Candida* vaginitis at least once in their lives and 70% of AIDS patients manifest oropharyngeal candidiasis (Calderone, 2001). In ICUs, the rate of fungal infections is on the rise: rates of *Candida* bloodstream infections range from 8-10%, however, mortality rates range from 29% to 40% (Clark, 2002). *Candida albicans* is the most common fungal pathogen in humans, followed by *Candida glabrata*, *Candida tropicalis,* and *Candida parapsilosis*, respectively (Kaufmann, 2006). 75% of all *Candida* infections in the 1980s were due to *Candida albicans*, however, more recently this rate has dropped to less than 60%. Despite the decrease in infections due to *C. albicans*, fungal infection overall remains a serious problem because there has been a parallel increase in antifungal resistant species such as *Candida glabrata* from 2% to 26%, *Candida parapsilosis* from 10% to 20%, and *Candida tropicalis* from 2% to 24% (Cappelletty, 2007). There are many factors that may explain this trend including geographical location, age of individual, patient population studied, and the use of fluconazole. *Candida glabrata* has been observed more often in patients older than 60 years and in centres caring for leukemia patients or patients who have received stem cell

transplants (Kauffman, 2006). *C. glabrata* is often resistant to fluconazole which is the drug most commonly used to treat candidemia, perhaps explaining the rise in occurrence of this species (Groll, 2002). This increase in the frequency of infections by fluconazole resistant species emphasizes the need to expand the armoury of antifungal drugs.

1.1.3 The economics of antifungal therapy

Economics offers an additional reason to search for novel antifungal therapies. Fluconazole will soon be off-patent which will allow generic pharmaceutical companies to develop generic fluconazole drugs and fluconazole derivatives. Efforts and budgets will thus be put towards the synthesis of modified fluconazole drugs instead of searching for new antifungals, for new targets. As companies do not want to incur the costs of drug discovery and the time and cost burdens of clinical trials, it will be less costly for them to put slightly modified azoles onto the market as new drugs instead of developing new strategies to combat fungal infections. Since pharmaceutical companies are driven by profits, they will strive to make the drugs which will be most profitable for them and not necessarily the drug discoveries which would be most beneficial for patients.

1.2 Current antifungal therapies

Fungal pathogens are functionally similar to human cells; this poses a challenge in the identification of effective drugs. Compounds that disrupt central cellular functions in the pathogen can cause similar disruptions in the host. For example, promising antifungals such as cycloheximide and rapamycin are also inhibitors of the same targets, protein synthesis and the mammalian target of rapamycin (mTOR) pathway respectively, in mammalian cells. There are currently three predominant classes of antifungal therapies on the market: echinocandins, polyenes, and azoles/triazoles. Currently antifungal compounds are directed at a very limited number of targets because fungi have proven to be target deficient which adds

to the challenge of antifungal discovery. These targets are primarily the cell membrane in the case of the azoles and amphotericin B, and in the case of the echinocandins, the cell wall (Gallagher, 2004).

1.2.1 Echinocandins; caspofungin

β-1,3-D-glucan synthase is responsible for the biosynthesis of the major cell wall biopolymer. Echinocandins inhibit β-1,3-D-glucan synthase by acting as a non-competitive inhibitors. They cause cell wall damage resulting in cell death, and thus they have fungicidal activity against *Candida* (Wagner, 2006, Cappelletty, 2007). The integrity of the fungal cell wall is essential, since without it fungi cannot survive. The wall is an extracellular matrix with a layered organization consisting of an outer layer of glycoproteins and an inner layer of carbohydrate polymers including glucan, chitin, and galactomannan (Perlin, 2007). Because the fungal cell wall is essential and composed of components that have no mammalian counterpart, the enzymes responsible for their synthesis provide potential targets for highly selective antifungals.

The target of echinocandins in *C. albicans* is Fks1, a 215-kDa integral membrane protein that is the major subunit of glucan synthase (Perlin, 2007) (Figure 1A). The first echinocandin drug to be FDA-approved was caspofungin in 2003. Since then, two other echinocandins have been FDA approved: micafungin and anidulafungin. Micafungin and anidulafungin have similar minimum inhibitory concentrations (MICs) which are lower than that of caspofungin (Cappelletty, 2007). Echinocandins have low toxicity to humans, rapid fungicidal activity against most isolates of *Candida* and they have predictable, favourable pharmacokinetics allowing for once a day dosing (Denning, 2002).

Common side effects associated with echinocandins are gastrointestinal effects such as nausea, vomiting, and diarrhea, but this occurs in less than 7% of patients. Caspofungin

Figure 1. Commonly used antifungals and their drug targets

A. Glucan synthase complex is responsible for producing 1,3-β-D-glucan chains which are essential for cell wall structure. Caspofungin targets α-1,3-mannosyltransferase encoded by the gene *FKS1*.

B. FCZ targets the *ERG11* gene product, cytochrome P450-dependent lanosterol 14-α-demethylase, in the ergosterol biosynthetic pathway. Amphotericin B is depicted inhibiting its target: ergosterol.

A.

UDP-glucose

1,3-β-D-glucan chains

Glucan synthase complex

FKS3- function unknown

RHO1- regulator of *FKS1* and *FKS2*

FKS2- chitin synthase

FKS1 – α-1,3-mannosyltransferase

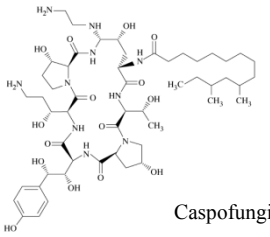

Caspofungin

B.

2 acetyl-CoA

Squalene

Squalene monooxygenase : *ERG1*

(S)-2,3-epoxysqualene

2,3-oxidosqualene lanosterol cyclase: *ERG7*

lanosterol

Cytochrome P450 lanosterol 14α-demethylase: *ERG11*

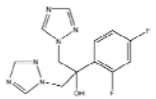

Fluconazole

4,4-dimethyl-cholesta-8,14,24-trienol

C14-sterol reductase: *ERG24*

4,4-dimethyl-8,24-cholestadienol

ergosterol

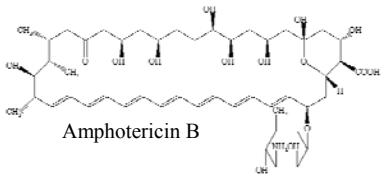

Amphotericin B

has a higher frequency of liver-related symptoms, infusion related pain and phlebitis than micafungin and anidulafungin (Cappelletty, 2007). A negative aspect of echinocandins at this point is their restricted antifungal spectrum which could be overcome by the newly arising pathogens being identified with the increasing population of immunocompromised patients (Morris, 2006). Because the echinocandins have only been on the market for a short period of time, resistance mechanisms have not been elucidated. A possible resistance mechanism has been suggested to be through mutation of the *FKS1* gene because laboratory derived mutants have demonstrated high-level *in vitro* resistance to lipopeptides (Ghannoum, 1999). However, the only immediate drawback to echinocandins is their cost.

1.2.2 Polyenes; amphotericin B

Polyenes and azoles/triazoles target the ergosterol pathway. The polyenes are fungicidal but toxic to the host, azoles/triazoles are fungistatic and more vulnerable to resistance (Perlin, 2007). Polyenes such as amphotericin B act by increasing the permeability of the cell membrane by targeting ergosterol in the membrane and forming a pore that leads to potassium ion leakage (Gupta, 2003) (Figure 1B). Polyenes have been in clinical use for over 30 years and only in rare cases has resistance been found. This resistance is ascribed to cells which produce modified sterols which have a lower affinity for the polyene drugs (Ghannoum, 1999). Although polyenes are effective broad-spectrum antifungals, serious side effects occur when administered to humans; these include kidney damage, liver failure, cardiac arrhythmias, and cardiac failure. Attempts have been made to decrease the toxicity levels by modifying amphotericin B by incorporating it in lipid formulations. Although toxicity levels are lower with these lipid modifications, more drug is required to obtain the desired therapeutic effects (Razzaque, 2001). Recently, a group showed that the toxicity of amphotericin B is impacted by the presence of impurities (Cleary, 2007). They suggest that

using lipid formulations of pure amphotericin B could greatly decrease the levels of toxicity. Clinical trials have yet to be performed to determine if this reduction in toxicity is observed. The use of amphotericin B is restricted to patients with severe fungal infections because of its toxicity and cumbersome administration (Verduyn Lunel, 1999).

1.2.3 Azoles; fluconazole

Azoles are fungistatic antifungals which inhibit the synthesis of ergosterol, a major and essential plasma membrane sterol. They function by targeting Erg11p, a cytochrome P450-dependent enzyme lanosterol 14-α-demethylase (White, 1998) (Figure 1B). At the molecular level, nitrogen molecules in the azole ring form a complex with the heme iron component of the cytochrome group, resulting in the inhibition of the enzyme (Yoshida, 1987). The ergosterol biosynthetic pathway converts acetic acid to ergosterol, using largely the same enzymes as in the mammalian biosynthesis of cholesterol. Although 14-α-sterol demethylase is also involved in mammalian cholesterol synthesis, azoles are therapeutic because they have a much greater affinity for the fungal CYP450 enzyme than the human CYP450 enzyme (Gupta, 2003).

Fluconazole (FCZ) is a widely-used broad-spectrum antifungal due to its good pharmacokinetic and toxicological profile. FCZ and the other azoles are the most commonly used drugs in the treatment of fungal infections; they are effective against most pathogenic *Candida* species (Grant, 1990) and do not have the serious side effects of amphotericin B. Because FCZ is fungistatic it arrests the growth of the pathogen but does not kill it. Ultimately, the host defences are responsible for clearing the pathogen from the bloodstream. Since pathogenic growth is blocked but the organism is not killed, it provides a strong potential for the development of resistance, and resistance to first generation azoles has already occurred (Anderson, 2003). Multidrug resistance mechanisms acquired by

Saccharomyces cerevisiae, *Candida albicans*, and other fungal species include modifications in the ergosterol biosynthetic pathway involving the over-expression or mutation of the azole drug target *ERG11* (Ribeiro, 2007), as well as over-expression of multidrug transporters (MacPherson, 2005, Akins, 2005, Albertson, 1996, Morschhauser, 2007, Perea, 2001). Furthermore, the inability to clear the pathogen in immune compromised patients results in fungal persistence and cycles of infection. Given the fact that the patients most susceptible to fungal infection are immune compromised, the need to find fungicidal therapies is paramount.

1.3 Combination therapies

One approach to the identification of new fungicidal treatments is to explore drug combination therapy (Marr, 2004, Fitzgerald, 2006). This approach has great precedent in the antibacterial field where, for example, the individually bacteriostatic type A (quinupristin) and type B (dalfopristin) streptogramin antibiotics are bactericidal when administered in combination (Moellering, 1999). This formulation has formed the basis for the antibiotic Synercid, approved in 2000. Other examples of successful combination therapy include Bactrim (trimethoprim-sulphamethoxazole) (Hubbard, 2003) as well as combinations of 3-4 antibiotics for treatment of infection caused by *Mycobacterium tuberculosis*, and the use of AZT and 3TC for control of HIV replication (Larder, 1995).

This approach is highly applicable to fungal infections as well. Clinically, the use of combination antifungal therapy is on the rise. First introduced in the 1970s for *Cryptococcal meningitis* (Bennett, 1979), antifungal combinations are becoming increasingly popular for the treatment of opportunistic mycoses. The major advantage of such combinations is enhanced antifungal activity that exceeds the effects of individual compounds in a synergistic interaction (Lewis, 2001, Kontoyiannis, 2003). Administration of multiple antifungal agents,

either concomitantly or sequentially, can increase treatment efficacy, decrease the selection for resistant strains, and reduce the toxicity associated with a single drug (Kontoyiannis, 2003, Fitzgerald, 2006). Combination therapy on fungi may result in one of three outcomes: indifferent growth, synergism or antagonism (Figure 2). Indifferent growth occurs when there is no synergism between the drugs and cells are affected by the combined individual ability of each drug. Synergism is described as a combined growth inhibition which is greater than the sum of the effect of each drug individually. Antagonism is a negative interaction observed where the combined effect of the drugs is less than when the drugs are tested separately. Identifying synergistic combinations has been a challenge because most antifungal combinations exhibit indifferent growth *in vitro* and in animal models of infection (Kontoyiannis, 2003).

Combination therapy has been studied using FCZ and cyclosporine A or FK506 (Onyewu, 2003). An assay using FCZ and cyclosporine A on a murine model of *C. albicans* keratomycosis provided more effective treatment compared to FCZ monotherapy (Onyewu, 2006). In using combination therapy, compounds identified to act synergistically with FCZ, rendering it fungicidal, could be used to effectively treat fungal infections. There has been a strong need for the development of techniques in the high-throughput identification of synergistic antifungal combinations. Here, we combine the necessity for high-throughput identification of synergistic antifungal combinations with the search for fluconazole synergistic fungicidal compounds with the development of a novel reporter assay.

1.4 Identification of novel antifungals

Recent developments in fungal genomics have provided the new tools for the development of antifungal compounds. The genome sequences of fungal pathogens can be compared with mammalian and other fungal genomes, and then pathogen specific targets can

Figure 2. Possible outcomes of combination therapy using two agents (adapted from Cuenca-Estrella, 2004).

Demonstration of combinations of two drugs diluted in two-fold increments. The shading in the figures on the right represents visible growth after spotting cultures on agar media and monitoring cell recovery. Combining two drugs for fungal treatment provides one of the following outcomes:

a) Indifferent or additive effect. The lack of growth is due to the combined ability of each drug to affect the cells.
b) Synergy. The growth inhibition effect is greater than the sum of the drugs' individual effects.
c) Antagonism. The combined effect of the drugs is less than when the drugs are tested individually.

A.

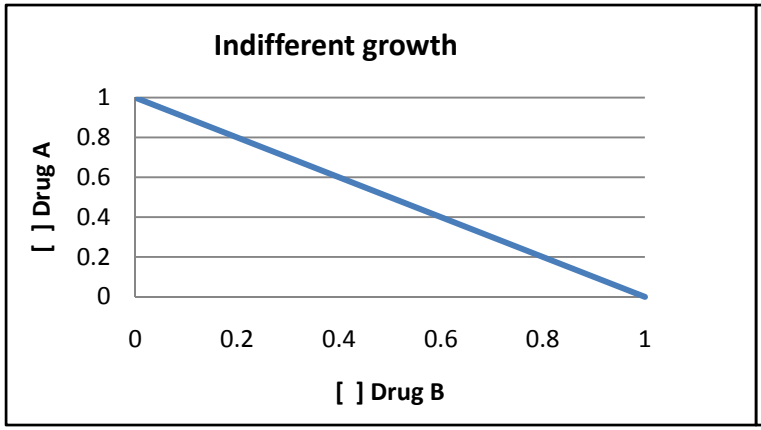
Indifferent growth
[ ] Drug A
1
0.8
0.6
0.4
0.2
0
0
0.2
0.4
0.6
0.8
1
[ ] Drug B

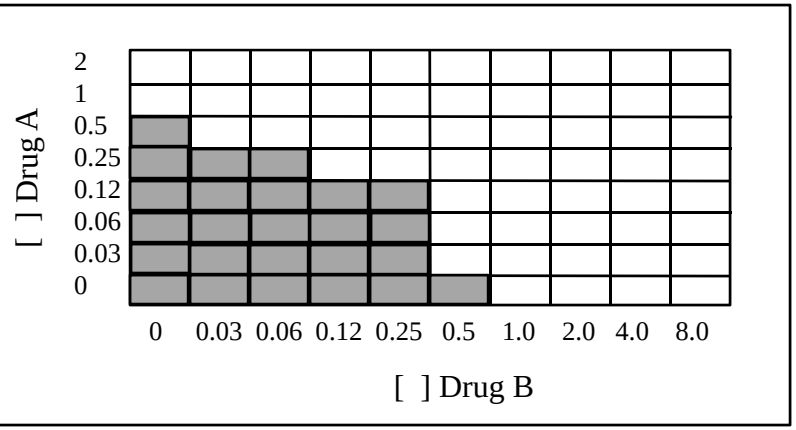
[ ] Drug A
2
1
0.5
0.25
0.12
0.06
0.03
0
0
0.03
0.06
0.12
0.25
0.5
1.0
2.0
4.0
8.0
[ ] Drug B

B.

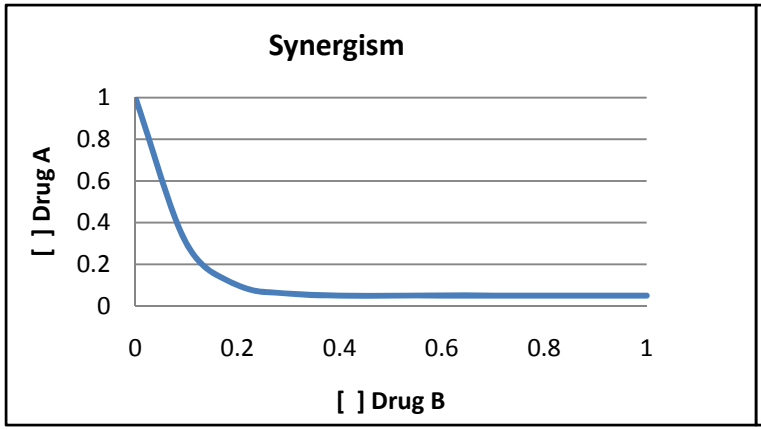
Synergism
[ ] Drug A
1
0.8
0.6
0.4
0.2
0
0
0.2
0.4
0.6
0.8
1
[ ] Drug B

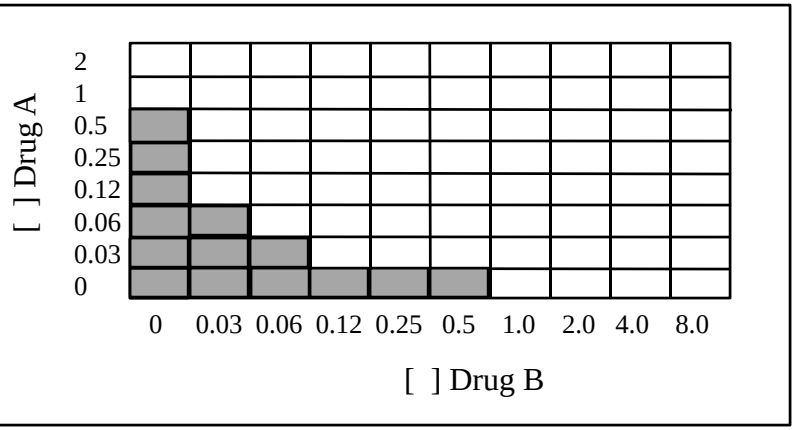
[ ] Drug A
2
1
0.5
0.25
0.12
0.06
0.03
0
0
0.03
0.06
0.12
0.25
0.5
1.0
2.0
4.0
8.0
[ ] Drug B

C.

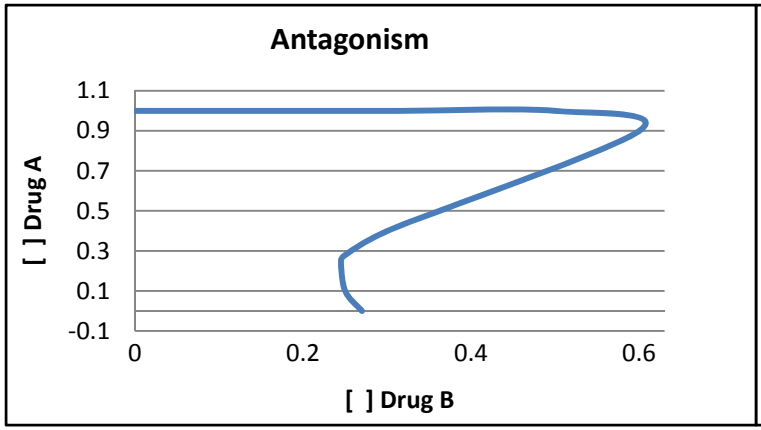
Antagonism
[ ] Drug A
1.1
0.9
0.7
0.5
0.3
0.1
-0.1
0
0.2
0.4
0.6
[ ] Drug B

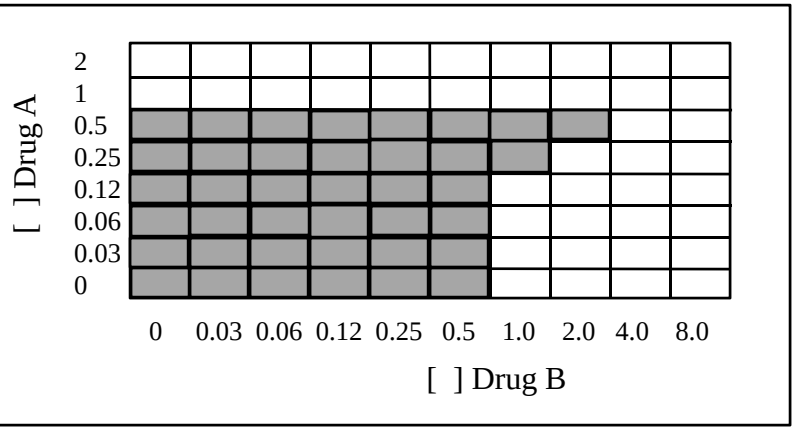
[ ] Drug A
2
1
0.5
0.25
0.12
0.06
0.03
0
0
0.03
0.06
0.12
0.25
0.5
1.0
2.0
4.0
8.0
[ ] Drug B

be used in high throughput screens. This approach has been facilitated by the large-scale generation of gene knockouts (Enloe, 2000) and the continuing characterization of the phenotypes of these mutants. This project develops a new strategy to antifungal discovery that couples a genomic approach with classical pharmacology. It uses the fungistatic compound FCZ in a chemical genetic screen for new targets that make the compound fungicidal.

1.4.1 Rationale

Our goal is to identify and characterize novel antifungal targets and discover new compounds that act synergistically with FCZ rendering it fungicidal. The underlying hypothesis to the approach taken is that there are yeast genes that are required to maintain cell viability in the presence of the fungistatic compound FCZ. These genes would then themselves be ideal targets for the screening of new compounds and the development of combination therapeutics with FCZ, creating a fungicidal pair. If a compound could be identified which targets an essential gene in fluconazole survival, then the combination of both compounds should be lethal to fungal cells.

In preliminary work, a screen was developed which used a concentration of FCZ that arrests growth of the wild type yeast strain but does not lead to significant cell death during the time of the experiment. This assay was then used to test the set of haploid yeast strains generated by the Yeast Genome Deletion Project which contain deletions of each of the 4757 non-essential genes (Jorgensen, 2002). After thorough characterization of the initial hits, twenty-three genes were identified to be essential for cell survival in the presence of FCZ. This set of genes was termed FCZ-fungicidal. As the deletion of a gene is akin to the functional inhibition of its protein product, the encoded proteins represent potential new targets for combination drug therapy with FCZ. The organism used in these studies as a

model for fungal pathogens was *Saccharomyces cerevisiae* due to its ease of manipulation for setting up the assay.

In the identification of compounds which act synergistically with FCZ, a unique strategy was used (Figure 3). The reasoning behind this approach is that if a compound is found to mimic the FCZ-fungicidal deletion strains, either by blocking the gene or protein's function, the combination of the compound and FCZ should be lethal to yeast cells. Microarray analysis was performed on the twenty-three FCZ-fungicidal strains compared to the wild type strain (Figure 3 I). From the expression profiles generated, highly up-regulated genes which had low expression in the wild type strain were identified and chosen to generate a growth reporter (Figure 3 II). The promoter of a significantly up-regulated gene, *FIT2*, was used to control the production of the *HIS3* gene in the reporter. This reporter is only activated in the absence of some FCZ-fungicidal genes and is not activated in the wild type strain (Figure 3 III). The growth reporter was then used to screen the Sigma LOPAC compound library, containing many pharmacologically active compounds, for compounds which would activate the reporter, indicating the loss of function of one of the genes determined to be essential in the presence of FCZ (Figure 3 IV). Activation of the reporter by a compound is detected by cell growth in media lacking histidine and containing 3-aminotriazole (3-AT, a competitive inhibitor to histidine). Diphenyleneiodonium chloride (DPIC) robustly and reproducibly activated the *FIT2* reporter. Then, its ability to act synergistically with FCZ in both *Saccharomyces cerevisiae* and *Candida albicans* was proven using a checkerboard technique (Figure 3 V).

Here we demonstrate that this novel strategy identifies synergistic counterparts to FCZ which render it fungicidal to both *Saccharomyces cerevisiae* and *Candida albicans* while simultaneously identifying the drug target.

Figure 3. Strategy for the novel reporter assay.

A novel approach is used in identifying FCZ synergistic fungicidal compounds while simultaneously identifying their drug targets.

I. Microarray analysis is performed on 23 deletion strains whose deleted gene has been determined to be essential for cell survival in the presence of FCZ.

II. A growth reporter is constructed using the promoter of a gene identified to be highly up-regulated according to the microarray analysis.

III. Cells transformed with the reporter are tested for growth on media lacking histidine and containing 3-aminotriazole (3-AT, histidine competitive inhibitor). The reporter should only be activated in the absence of a FCZ-fungicidal gene and cell growth is only observed if the reporter is activated (H: haploid strain, D: heterozygous diploid strain).

IV. A compound library is screened with the reporter to identify drugs which activate it (cell growth is represented by red dots).

V. These hit compounds are tested for FCZ synergy by checkerboard analysis in both *Saccharomyces cerevisiae* and *Candida albicans*.

I

23 FCZ-fungicidal deletion strains

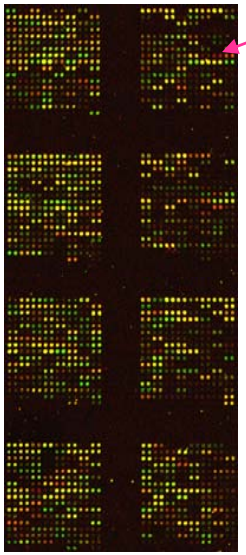

Microarray analysis

II

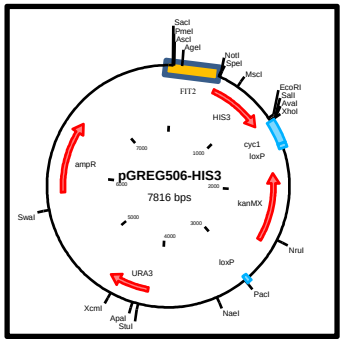

Construction of growth reporter (*HIS3*) under the control of a specifically upregulated gene

III

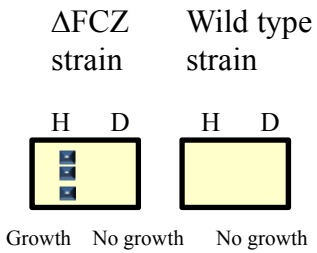

Specificity test for growth on histidine lacking media containing 3-aminotriazole (3AT)

IV

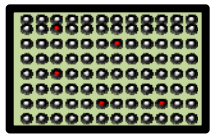

Compound library screened with reporter

V

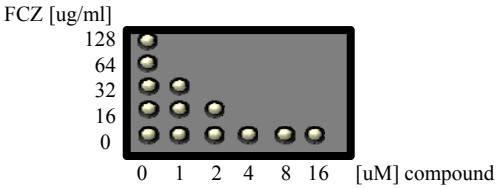

Synergy test between compound and FCZ in both *Saccharomyces cerevisiae* and *Candida albicans*

Chapter 2

Materials and Methods

2.1 Strains, media and plasmids

The *Saccharomyces cerevisiae* haploid strain BY4741 and the complete yeast deletion array collection in the BY4741 background were obtained from the American Type Culture Collection (ATCC). *S. cerevisiae* was cultured in rich media (YPD), synthetic complete media (SC), or synthetic drop-out media; for solid media, 2% agar was added (Table 1). A detailed list of the plasmids used in this study is provided in Table 2.

2.2 FCZ-fungicidal deletion strains

2.2.1 Fluconazole sensitivity screen

96-well plates containing the ATCC *S. cerevisiae* deletion strains were replicated with a 96-pin replicator (Boekel) to single-well Omnitray plates (Nalgene Nunc) containing agar YPD media and geneticin (200µg/mL) and, simultaneously, to plates containing agar YPD media and FCZ (85µg/mL). Fluconazole (Pfizer Limited, Sandwich, Kent, UK) was dissolved in dimethyl sulfoxide (DMSO). Plates were incubated at 30°C for 48 hours. Following incubation, cells on the YPD and FCZ plates were replicated to fresh YPD plates (without FCZ) and incubated at 30°C for 48 hours. Plates were scored for deletion strains that were unable to grow after exposure to FCZ.

2.2.2 Rhodamine 123 and FUN 1 staining

The Rhodamine 123 (Invitrogen) staining was performed as described by Egner *et al*. (Egner, 1998). Cells were monitored for 2 hours after washing out the dye. This dye was used in identifying defects in Pdr5p mediated detoxification; characterized by prolonged intracellular accumulation of the dye after its removal from the media.

Staining with FUN 1 was performed to investigate the accumulation of cylindrical intravacuolar structures (CIVSs) in the vacuole. The manufacturer's protocol (Invitrogen)

Table 1 List of media used.

Medium	Components
2YT	1% yeast extract, 1.6% tryptone, 0.5% sodium chloride
2YT and ampicillin	1% yeast extract, 1.6% tryptone, 0.5% sodium chloride, 50mg/mL ampicillin
YPD	1% yeast extract, 2% peptone, 2% dextrose
YPgal	1% yeast extract, 2% peptone, 4% galactose
Synthetic complete (SC)	0.67% yeast nitrogen base, 2% dextrose and 15mg/L of amino acids
Synthetic complete 4% galactose (SCgal)	0.67% yeast nitrogen base, 4% galactose and 15mg/L of amino acids
-URA synthetic drop-out dextrose (ura^-)	0.67% yeast nitrogen base, 2% dextrose and 15mg/L of amino acids without uracil
-URA synthetic drop-out galactose (ura^-gal)	0.67% yeast nitrogen base, 4% galactose and 15mg/L of amino acids without uracil
-HIS synthetic drop-out dextrose (his^-)	0.67% yeast nitrogen base, 2% dextrose and 15mg/L of amino acids without histidine
-HIS synthetic drop-out galactose (his^-gal)	0.67% yeast nitrogen base, 4% galactose and 15mg/L of amino acids without histidine
-LEU synthetic drop-out dextrose (leu^-)	0.67% yeast nitrogen base, 2% dextrose and 15mg/L of amino acids without leucine
YPDU	1% yeast extract, 2% peptone, 2% dextrose, 2% agar and 50mg/L uridine

Table 2 List of plasmids and strains used.

Plasmids	Description	Reference
pGREG 506-HIS3	*GAL1-HIS3-URA3-KanMX^R-Amp^R* Cen plasmid, URA and HIS3 marker	Jansen, G., 2005
pGREG 506-HIS3 FIT2	*FIT2 -HIS3-URA3-KanMX^R-Amp^R* Cen plasmid, URA and HIS3 marker	This study
pGREG 486	*GAL1-HIS3-URA3-KanMX^R-Amp^R*	Jansen, G., 2005

Strain	Genotype	Reference
Saccharomyces cerevisiae wild type BY4741	*MAT**a** his3Δ1 leu2Δ0 met15Δ0 ura3Δ0*	Brachmann, 1998
Candida albicans wild type strain SC5314	Wild type	Gillium, A.M., 1984

was followed. Briefly, cells were stained for 30 min at 30°C, then the dye was removed from the media, and cells were resuspended in fresh staining buffer without dye and further incubated at 30°C for an hour before they were examined microscopically.

2.3 Complementation assay

To demonstrate that FCZ sensitivity was dependent on the particular gene deletion and not on an acquired secondary mutation, the deletion strains were transformed with plasmids harbouring their respective deleted genes expressed from the galactose inducible *GAL1* promoter (Gelperin, 2005). The plasmid DNA was isolated from the *E. coli* host using the Qiaprep miniprep (Qiagen). The extracted plasmid DNA was confirmed to contain the appropriate gene by digestion with restriction enzymes Age I and Nar I (New England Biolabs). Plasmids giving questionable digests were confirmed by sequencing. Plasmids were transformed into their respective deletion strains. The transformants were incubated in two sequential overnight cultures. Cells were diluted and treated with FCZ concentrations ranging from 16 to 128µg/mL and then incubated at 30°C for 24 hours. After incubation, 2µL of cultures were spotted onto fresh YPD plates, incubated at 30°C for 2 days, and scored for growth. The complementation test was performed under both inducing (SCgal) and non-inducing (SC) conditions.

2.3.1 Yeast transformation

Fresh yeast cells derived from a single colony were scraped from an agar plate and added to 100µL of 44% polyethylene glycol (PEG) in 0.1M lithium acetate. 1µL of 5mg/mL salmon sperm DNA (Invitrogen), previously boiled and incubated on ice, and 5uL plasmid DNA were added to the cell suspension. (For *in vivo* recombination, 15µL of PCR product and 10µLof digested plasmid were added.) The mixture was mixed and incubated a minimum

of 4 hours at 30ºC. The cells, which were settled to the bottom of the Eppendorf tubes, were plated on selective media and incubated for 3 days.

2.3.2 Plasmid DNA extraction from yeast

Plasmid DNA extraction from yeast was performed using the QIAprep Miniprep (Qiagen). Incubation for one hour with a Zymolase (MP biomedicals, LLC) solution (5mg/mL zymolase in 1.2M sorbitol/50mM EDTA) was used to digest the cell wall. Then, the standard Qiaprep protocol was used to extract the DNA. The yield for these extractions was low (ng).

2.3.3 Bacterial transformation for plasmid regeneration

0.5µL of plasmid DNA was inoculated into approximately 125µL of *E. coli* top 10 competent cells which were previously thawed on ice. The cells were incubated on ice for 10 minutes, followed by a 30-second incubation at 42°C, and finally they were added to 2 tubes containing 5mL of 2YT media and incubated overnight. Cells were plated on agar 2YT media and ampicillin (50mg/mL) and allowed to grow overnight. Single colonies were picked, inoculated in 4mL 2YT media and ampicillin (50mg/L) and were allowed to grow overnight. Plasmid DNA was extracted from *E. coli* using QIAprep miniprep (Qiagen).

2.4 Microarray experiments

2.4.1 Cell preparation

The RNA extraction protocol from Paul Jorgensen and Theo Goh from the Ontario Cancer Institute, modified by Babette Schade and Christina Kast was followed. Briefly, tubes containing 5mL of YPD media were each inoculated with either an ATCC deletion strain or wild type strain from -80°C stocks and allowed to grow overnight at 30ºC with shaking. The next day, 100mL of YPD was inoculated with cells from the previous overnight culture and

allowed to grow overnight at 30ºCwith shaking. The overnight culture was then diluted to an 0.05 optical density value at wavelength 600nm (OD_{600}) in a final volume of 400 mL of YPD. Cells were returned to the 30ºC shaking incubator and allowed to grow 6-8 hours to a final OD_{600} value of approximately 0.8. The culture was then transferred into 50mL falcon tubes. Cells were pelleted by centrifugation and flash-frozen in liquid nitrogen.

Microarray analysis was performed on deletion strain Δ*pdr5* treated with FCZ. The identical inoculation and incubation protocol was used as described above, however, on the last day, strains were grown to an OD_{600} of 0.6 in 300mL of YPD. 500mg of FCZ were dissolved in 100mL of YPD. Then 100mL of YPD were added to the wild type and 100mL of YPD and FCZ were added to the Δ*pdr5* deletion strain, cells were pelleted after 90 and 180 minutes of treatment at 30ºC in the shaking incubator.

2.4.2 RNA extraction and purification

The RNA extraction protocol used involves adding hot phenol immediately after the addition of a 50mM sodium acetate and 10mM EDTA (SAB) buffer to the frozen pelleted cells without allowing for a thawing period. This method prevents RNA degradation during thawing. The tubes containing the cells and phenol were allowed to incubate in a 65°C water bath for one hour. More RNA was obtained with longer hot phenol incubation. Samples were vortexed and then centrifuged, the top aqueous layer containing the RNA was kept throughout the subsequent extractions involving phenol/chloroform and finally chloroform/isoamyl alcohol. RNA was allowed to precipitate overnight in ethanol and 3M sodium acetate. After washing and resuspending the RNA in diethylpyrocarbonate (DEPC)-treated (Sigma) double distilled water, the RNA was diluted 1:10 and was quantitated using the nanodrop. RNA was qualitated by running a 1% RNase free agarose gel, loading 1µg of RNA per lane. 1X MOPS (Bioshop) buffer was used to make the gel and as the running

buffer. The gel apparatus was made RNase free using RNase zap (Ambion) and rinsing with DEPC-treated double distilled water. RNA was stored at -80°C. Total RNA purification was performed using the RNeasy kit (Qiagen).

2.4.3 cDNA microarray analysis

The protocol for the microarray analysis was obtained from Daniel Dignard at the Biotechnology Research Institute (BRI). Briefly, probes for microarray analysis were prepared using 25-30μg of total RNA. The RNA was mixed with 100pmol of oligo dT, denatured at 70°C for 10 minutes and then chilled on ice. Cyanine labelled cDNA was synthesized using Superscript II reverse transcriptase (Invitrogen) and cyanine 3-dCTP or cyanine 5-dCTP (Perkin Elmer). Dye swap analysis was performed by reversing the dyes used to label the RNA samples. cDNA microarrays from the University Health Network (UHN) were used. Microarrays were pre-hybridized using salmon sperm DNA (Invitrogen) and baker's yeast tRNA (Sigma). Hybridization of the probes in digoxigenin (DIG) easy hybridization buffer (Roche) to the pre-hybridized microarrays was performed at 42°C for 16 to 20 hours. After washing the microarrays in buffers made up of sodium chloride and sodium citrate (SSC) and sodium dodecyl sulphate (SDS), they were scanned on a ScanArray Lite Microarray Scanner (Packard BioScience Biochip Technologies).

2.5 Microarray bioinformatics analysis

2.5.1 Data pre-processing

For each mutant versus wild type (WT) array, first, background subtraction was performed; subtracting the measured local background intensity from the measured spot intensity. Second, the array data was processed with spatial LOWESS (LOcally WEighted Scatterplot Smoothing) normalization to remove the dependence of fold-change on spatial trends in the array (e.g. caused by artifacts). Third, MA LOWESS normalization was applied;

removing the dependence between fold change (represented by the log-ratio $M= \log_2(R) - \log_2(G)$) and the intensity (represented by average intensity, $A= (\log_2(R) + \log_2(G))/2$ where R represents the red probe intensity and G represents green probe intensity). Fourth, quantile normalization to the WT intensity distribution was performed; adjusting the WT intensity distribution from a new array to match the WT reference distribution in order to facilitate comparison between different arrays. The reference WT intensity distribution was computed from the pre-processed red and green intensity distributions of the WT versus WT reference arrays. For each spot, the median of all intensity measurements was used to form reference distribution. Only the WT intensity distribution in a mutant versus WT array was quantile normalized to the reference distribution. Finally, scale normalization was performed to again make different arrays more comparable. Scale normalization ensures that all array profiles have log-ratios that deviate from the median in roughly the same way. Specifically, the log-ratios were normalized such that each array has the same median-absolute-deviation (MAD); deviation here refers to the difference of the log-ratio of a gene from the median log-ratio of a given array. Since it is generally assumed that the majority of genes are not differentially expressed in any comparison, the MAD for each array should be close to zero.

A similar pre-processing approach was used for the WT-WT reference pool of arrays. However, there were some modifications. Spatial LOWESS normalization was not necessary because any minor array artifacts were taken into account during background subtraction. Also, quantile normalization was performed between arrays (not to a reference) and the intensity distribution of each channel of each WT-WT chip was made to be the same (the average distribution).

2.5.2 Computation of the FCZ-fungicidal expression profile correlation

An agglomerative clustering method was used in the analysis of the FCZ-fungicidal profiles. This method adds edges individually, at each step merging the two clusters that are closest together. The measure of closeness is computed with Ward's method, which merges candidate clusters that have the lowest variance (Ward, 1963). The edge # indicates the order in which the edges/branch points were formed. Approximately Unbiased (AU) p-value and Bootstrap Probability (BP) p-value were used to compute the statistical significance of the clustering. A p-value of 0.01 provides 99% statistical significance, thus the more elevated the value, the more significant the cluster.

2.5.3 Differential Expression Analysis

LIMMA (LInear Models for MicroArray data) was used to determine statistically significant differential expression. The Benjamini and Hochberg method for multiple-test correction was applied and an adjusted $p < 0.05$ cut-off was used to indicate significant differential expression. Genes that were significantly over-expressed in a mutant strain compared to the wild type, but that were also expressed at low levels or not at all in the wild type, were identified. Such a gene is a candidate for reporting the down-regulation of the FCZ-fungicidal gene with which it is associated. A gene that had an intensity below the mean intensity in the WT reference distribution was considered to be expressed at a low level. Candidate reporter genes were restricted to genes that showed a fold-change of >2 to facilitate hit detection in the drug screens. Moreover, genes annotated to stress response (according to www.geneontology.org) were filtered out since they were likely to be non-specific reporters.

2.5.4 Assessing the performance of candidate reporters from existing data

For each candidate reporter gene, false positive and false negative rates were computed based on its expression and the expression of its genes-to-report-on (i.e. target FCZ-fungicidal genes) in a yeast expression profiles collected from the literature. There were 528 profiles in total, and 305 of them had associated p-values. The p-values for each profile were multiple-test corrected using the Benjamini and Hochberg method. A gene was considered significantly under-expressed compared to wild type if its fold-change was <= 0.5, and significantly over-expressed if its fold-change was >=2. If a p-value was available and used in the analysis, another constraint was applied: adjusted $p < 0.05$.

2.6 *FIT2* reporter

The *FIT2* promoter with flanking regions homologous to the pGREG506-HIS3 plasmid was generated by polymerase chain reaction (PCR) using the following primers:

Forward:

5'-CGCAATTAACCCTCACTAAAGGGAACAAAAGCTGGAGCTCCTGACTCAACGTTGATGATGCGAGTAGTGGG-3'

Reverse:

5'-GGTTTCATTTGTAATACGCTTTACTAGGGCTTTCTGCTCTGTCATTATTATTGTTTTGTGATGGCTTTATGATAGAC-3'

The plasmid pGREG506-HIS3 was digested with restriction enzymes Asc1 and Spe1 (New England Biolabs), excising the *GAL1* promoter, to allow for more efficient *in vivo* recombination. Then the Δ*vma4* deletion strain was transformed with 10µL of the digested pGREG506-HIS3 and 15µL of the *FIT2* promoter PCR product, plated on ura$^-$ agar plates and incubated at 30ºC for three days. This allowed for *in vivo* recombination of the pGREG506-HIS3 lacking the *GAL1* promoter and the *FIT2* promoter PCR product creating the *FIT2* reporter gene. The Δ*vma4* deletion strain with the reporter was mated to a BY4742 *MATα* strain. The haploid and diploid strains, were then replica plated on agar media: his$^-$, his$^-$gal, ura$^-$ and his$^-$ containing 4 different concentrations (5mM, 10mM, 15mM and 40mM)

of 3-AT, a competitive inhibitor of histidine, and allowed to incubate at 30 ºC for two days. The plasmid DNA was isolated from haploid strains whose corresponding diploid strain did not grow in the presence of 3-AT. The plasmid DNA was then amplified and confirmed to be the expected construct by sequence analysis. The plasmid DNA was transformed again into the Δ*vma4* deletion strain as well as Δ*vma13,* Δ*vma22,* Δ*tps2,* Δ*gcs1,* homozygous diploid Δ*vma22* and the wild type strain.

2.6.1 Apotransferrin assay

An assay was performed using the iron chelator apotransferrin (Cedarlane labs). Various concentrations of apotransferrin were used, 0.2, 1, 2, 4, 6, 8 mg/mL, in both his^- and his^- 15mM 3-AT media. The apotransferrin assay was tested with the wild type strain containing the *FIT2* reporter, the Δ*vma4* deletion strain containing the reporter and the Δ*vma4* deletion strain containing the pGREG506-HIS3 plasmid without a promoter. These strains were incubated for 46 hours at 30ºC and growth was monitored by measuring OD_{600}.

2.7 Reporter screen

The *FIT2* reporter in the wild type strain was used to screen the entire Sigma LOPAC (Library Of Pharmacologically Active Compounds) library (Sigma-Aldrich) that contains 1280 compounds of a diverse variety. Cells previously grown overnight in ura^- media at 30ºC were inoculated at a cell density of 12000 cells per well in both his^- media and freshly prepared his^- 15mM 3-AT media. The his^- media was used as a control to determine if the compounds were toxic to the cells. This experiment was performed using a Biomek FX (Beckman Coulter) robot. First, 100µL of media were added to 96-well plates (NUNC). Then, 0.1µL of compound (2mM) dissolved in DMSO was added using the robot pin tool. Finally, 100µL of culture corresponding to 12 000 cells were added. The 96-well plates were incubated for 46 hours at 30ºC and growth was monitored by measuringOD_{600}.

The *FIT2* reporter in the Δ*vma4* deletion strain was used as a positive control. The pGREG506-HIS3 plasmid without any reporter in the Δ*vma4* deletion strain was used as a negative control. The untreated wild type strain with the *FIT2* reporter was also included as a control in the screen.

Another screen using the Sigma LOPAC library was performed using the same approach as described above except that 6000 non-transformed wild type cells were added to each well and 10μg/mL of FCZ was added to the media.

2.8 Checkerboard analysis

In determining if two compounds act together synergistically, additively, or antagonistically, a technique created by Georges M. Eliopoulos called checkerboard is used (Cuenca-Estrella, 2004). The assay is set up such that from left to right on a 96-well plate, increasing concentrations of drug A are added to the wells and from top to bottom on the plate, increasing concentrations of drug B are added. Cells are treated for 24 hours at 30ºC, then 2μL of culture are spotted on YPD agar media. The plates are incubated for two days at 30ºC before cell recovery is assessed (Figure 2). DMSO checkerboard controls are also performed to ensure that the effect observed is solely due to the compound and not the solvent it is dissolved in.

2.8.1 Checkerboards verifying synergy in *Saccharomyces cerevisiae*

Wild type cells were grown overnight in SC media at 30ºC. 6000 wild type cells in a volume of 33.3μL were then added to each well in a 96-well plate (NUNC). 33.3μL of each FCZ and DPIC, previously dissolved in DMSO and diluted in SC media, were added to the wells providing final concentrations of 8 and 16μg/mL and two-fold dilutions ranging from 0.3μM to 5μM, respectively. 96-well plates were incubated at 30ºC for eleven days and cell recovery was monitored initially after 24 hours of incubation and then every 48 hours by

spotting 2µL of culture on YPD agar media. These plates were incubated for two days at 30ºC before cell recovery was assessed.

2.8.2 *Candida albicans* checkerboard analysis.

A single *Candida albicans* wild type SC5314 colony (from a freshly thawed 20% glycerol stock) was incubated overnight in 10mL YPDU media at 30°C. The following day, cells were diluted to an OD_{600} of 0.1 and returned to 30°C. At an OD_{600} between 1 and 1.5, the inoculum was diluted to provide a final concentration (including the volume of the drugs) ranging between $1x10^3$ and $3x10^3$ cfu/mL.

In a 96-well plate (Corning Inc.), 50µL of each DPIC and FCZ were added to 50µL of cells providing final concentrations of 20, 40 and 80µM of DPIC and two fold dilutions of FCZ ranging between 2 and 128µg/mL. The plates were incubated for 3 days at 30°C and cell recovery was monitored by spotting 2µL of culture on YPDU agar plates. Following 24 hours of incubation the spotted cultures were assessed for cell recovery.

2.9 Analysis of diphenyleneiodonium chloride

2.9.1 Screen to identify the diphenyleneiodonium chloride target

The SGA library containing strains from 3761 individually deleted genes was pinned onto YPD agar plates and incubated for 24 hours at 30ºC. This experiment was performed using a VersArray™ colony picker and arrayer system (BioRad ViRTEK). The library was then pinned onto synthetic complete media containing 450µM DPIC, incubated for 24 hours at 30ºC and colonies were scored for sensitivity. The screen was performed in parallel with DMSO control plates which was used as a reference when scoring for sensitivity. Sensitive strains were retested on agar plates containing 400µM, 450µM and 500µM using the same protocol as described above. Sensitive strains were also grown overnight at 30ºC in liquid SC

media, diluted and tested in SC liquid media containing DPIC concentrations ranging from 31.25uM to 500uM.

2.9.2 Assay used to determine if diphenyleneiodonium chloride targets *VMA* genes

6000 wild type cells previously incubated overnight at 30ºC in synthetic complete media were inoculated in three different media: synthetic complete 3% glycerol, synthetic complete pH 8 and synthetic complete supplemented with 50mM $CaCl_2$. DPIC was added to the media to provide final concentrations of 125μM, 250μM and 500μM. This experiment was performed in parallel with a DMSO control. Strains were incubated for 48 hours at 30ºC and then were scored for growth. After 3 days of incubation at 30ºC, 2μL of the cultures were spotted onto YPD agar media. The plate was incubated for 2 days at 30ºC and then cell recovery was assessed.

Chapter 3

Results

3.1 Identification of yeast genes required for viability in the presence of FCZ

Previous work involved screening the entire haploid yeast strain collection generated by the Yeast Genome Deletion Project, which contains the deletion strain of each of the 4757 non-essential genes, with a sub-lethal concentration of FCZ (Jorgensen, 2002). The hypomorphic strain for the essential gene *ERG11* was used as a control. Erg11p is directly targeted by FCZ which specifically inhibits its enzymatic activity in the ergosterol biosynthesis pathway. The hypomorphic *erg11* strain is expected to die in the presence of FCZ due to its compromised cellular quantities of the drug's target. The screen identified 22 strains, in addition to the *erg11* hypomorphic strain, which were unable to recover after exposure to FCZ (Table 3). These 23 strains were termed FCZ-fungicidal. The list of FCZ-fungicidal genes includes the pleiotropic drug pump *PDR5*, and genes from functional categories such as vacuolar functionality, chromatin modification, and transcriptional regulation.

Approximately one third of the FCZ-fungicidal gene products are directly involved in transcriptional regulation: the members of the SAGA complex and the mediator complex. The SAGA complex (Spt-Ada-Gcn5-acetyltransferase) is involved in transcriptional activation. Various factors are required to facilitate this process. In the cell, DNA is tightly packaged into nucleosomes where it is wound around histone proteins and inaccessible to the transcriptional machinery. In order for transcription to occur the nucleosomes must be perturbed at promoter regions and, in *Saccharomyces cerevisiae,* this remodeling process is performed by the SAGA complex. Among the FCZ-fungicidal genes, *ADA2*, *GCN5*, *NGG1,* and *SPT20* belong to the SAGA complex and, more specifically, all these genes interact together as part of the ADA complex (Eberharter, 1999). *GCN5* provides the histone acetyltransferase (HAT) activity to interact with the histones and render the DNA available to the transcription machinery. *ADA2* interaction with *GCN5* is necessary for the proper

Table 3 List of the FCZ-fungicidal genes. Gene descriptions from www.yeastgenome.org.

Systematic	Common	Gene Description	Localization
YDR448W	ADA2	Transcription coactivator, component of the ADA and SAGA transcriptional adaptor/HAT complexes	nuclear lumen
YGR252W	GCN5	Histone acetyltransferase, catalytic subunit of the ADA and SAGA histone acetyltransferase complexes	nuclear lumen
YDR176W	NGG1	Component of transcriptional adaptor and histone acetyltransferase complexes, the ADA complex, the SAGA complex, and the SLIK complex	nuclear lumen
YOL148C	SPT20	Subunit of the SAGA transcriptional regulatory complex, involved in maintaining the integrity of the complex	nuclear lumen
YDL185W	TFP1	Vacuolar H^+-ATPase V1 domain subunit A	vacuolar membrane
YOR332W	VMA4	Subunit of the V1 peripheral membrane domain of the vacuolar H^+-ATPase (V-ATPase)	vacuolar membrane
YHR039C-A	VMA10	Vacuolar H^+-ATPase subunit of the catalytic V1 sector, involved in vacuolar acidification	vacuolar membrane
YPR036W	VMA13	Subunit of the H^+-ATPase V1 domain; activator or a structural stabilizer of the V-ATPase	vacuolar membrane
YHR060W	VMA22	Functions in the assembly of the H^+-ATPase complex	ER membrane
YKL119C	VPH2	Functions in the assembly of the H^+-ATPase complex	ER membrane
YER155C	BEM2	Rho GTPase activating protein involved in the control of cytoskeleton organization and cellular morphogenesis	mitochondrion
YDL226C	GCS1	ADP-ribosylation factor GTPase activating protein, involved in ER-Golgi transport	ER-Golgi intermediate compartment, cytoskeleton
YDR129C	SAC6	Fimbrin, actin-bundling protein involved in the organization and maintenance of the actin cytoskeleton	actin cytoskeleton
YHR030C	SLT2	Serine/threonine MAP kinase involved in regulating the maintenance of cell wall integrity and cell cycle progression	Bud tip, nucleus
YCR081W	SRB8	Subunit of the RNA polymerase II mediator complex and RNA polymerase II holoenzyme	nuclear lumen
YPL042C	SSN3	Cyclin-dependent protein kinase, component of RNA polymerase II holoenzyme	nuclear lumen
YDL005C	MED2	Subunit of the RNA polymerase II mediator complex and RNA polymerase II holoenzyme	nuclear lumen
YHR007C	ERG11	Lanosterol 14-α-demethylase of the ergosterol biosynthesis pathway; member of the cytochrome P450 family	endoplasmic reticulum
YDL116W	NUP84	Subunit of the nuclear pore complex (NPC)	nuclear pore
YOR153W	PDR5	Plasma membrane ATP-binding cassette (ABC) transporter	plasma membrane, mitochondrion
YHR025W	THR1	Homoserine kinase required for threonine biosynthesis	unknown
YDR074W	TPS2	Phosphatase subunit of the trehalose-6-phosphate synthase/phosphatase complex	mitochondrion
YDR532C	KRE28	Localizes to the nuclear side of the spindle pole body and along short spindles	spindle pole body, cytoskeleton

function of the HAT activity (Candau, 1997). *SPT20* is required for transcription and for normal TATA-binding protein (TBP) function (Roberts, 1996, Baker, 2007). *NGG1* participates in gene activation and repression and is also required to interact with TBP for it to function properly (Saleh, 1997). Deletion of several different SAGA components results in reduced recruitment of RNA polymerase II to its promoters and lower transcription levels.

The mediator complex is involved in transcriptional regulation which is important for negative and positive control of transcription. It is capable of integrating multiple signals and processing regulatory information at the promoters of higher organisms (Kornberg, 2005). From the FCZ-fungicidal set of genes, *SRB8*, *SSN3*, and *MED2* are members of the mediator complex. *SRB8* and *SSN3* both undergo protein-protein interactions with *MED2*, while the latter is required for efficient recruitment of RNA polymerase II. *SRB8* is part of a negative regulatory module to the mediator complex; it is thought to play a predominantly negative role in transcription, however, it can play a positive role as well (Milgrom, 2005). *SSN3* functions in a cyclin-dependent kinase cyclin pair with *SSN8* and is identical to the member of the *SRB* suppressor family *SRB10* (Song, 1996). *SSN3* contributes to transcriptional repression of diversely regulated genes (Kuchin, 1995).

The pleitropic drug pump *PDR5* is the yeast homolog of the human multidrug resistance (MDR1) transporter and is regulated by the SAGA complex (Gao, 2004). It has been shown that the transcription of *PDR5* requires recruitment of the SAGA and mediator complexes to its promoter (Gao, 2004). Thus, with impaired activity of the SAGA or mediator complex may lead to Pdr5p not being produced in sufficient quantities to pump FCZ out of the cell. In previous work, Rhodamine 123 staining was used to assess Pdr5p activity in each of the FCZ-fungicidal strains. This fluorescent dye is specifically exported from the cell by Pdr5p and in its absence there is a continuous intracellular accumulation of the dye after washout (Egner, 1998). The results suggested that the deletion strains Δ*ada2*, Δ*gcn5*,

Δ*ngg1*, Δ*spt20*, Δ*srb8*, Δ*slt2*, Δ*pdr5,* and Δ*kre28* were unable to efficiently export the dye as compared to wild type controls. It should be noted that this experiment was not performed on the Δ*med2* deletion strain. These findings support the hypothesis that the members of the SAGA complex and some of the genes belonging to the mediator complex, among the FCZ-fungicidal genes, are required for the proper function of Pdr5p.

The FCZ-fungicidal set also contains six genes that encode subunits of the vacuolar proton-translocating ATPase (V-ATPase) complex. The V-ATPase is a highly conserved proton pump responsible for acidification of organelles such as the lysosome/vacuole, Golgi apparatus, and endosomes. Yeast mutants lacking subunits of the V-ATPase have been identified in multiple genomic screens for sensitivity to different forms of oxidative stress. (Milgrom, 2007) All eukaryotic V-ATPases are multi-subunit enzymes comprised of a complex of peripheral membrane proteins, V_1, attached to a complex of integral membrane proteins, V_0. It has been well documented that *vma* mutants exhibit poor growth on non-fermentable carbon sources, hypersensitivity to multiple drugs, and increased sensitivity to transition metals such as iron, copper, and zinc (Milgrom, 2007). Among the FCZ-fungicidal genes, *VMA1/TFP1*, *VMA4*, *VMA10*, *VMA13*, *VMA22,* and *VPH2* are part of the V-ATPase complex; the first four are part of the V_1 subunit whereas the latter two are localized in the endoplasmic reticulum and are part of the V_0 subunit.

In previous work each of the FCZ-fungicidal strains was stained with the fluorescent dye FUN 1 (www.invitrogen.com). When added to live cells the dye produces a green fluorescence when present in the cytoplasm until it accumulates in the vacuole where the fluorescence becomes red. In the vacuole, formation of compact cylindrical intravacuolar structures (CIVSs), producing the red fluorescence, requires plasma membrane integrity and metabolic capability. After washing out the dye, deletion strains Δ*gcn5*, Δ*vma1/tfp1*, Δ*vma4*, Δ*vma10*, Δ*vma13*, Δ*vma22*, Δ*vph2*, Δ*sac6*, Δ*srb8,* and Δ*kre28* were comprised of cells with a

mixture of red and green signals, whereas wild type cells only presented a red signal. All the V-ATPase deletion strains from the FCZ-fungicidal set demonstrated impaired deposit of the dye in the vacuole. This suggests that these strains might also be ineffectively depositing other compounds, such as FCZ, in the vacuole.

Genes *GCS1*, *SLT2*, *SAC6,* and *BEM2* are involved in maintaining and organizing the cell wall or cytoskeleton. *BEM2* and *SAC6* are genes involved in the organisation and maintenance of the cytoskeleton (Wang, 1995, Adams, 1991) whereas *GCS1* is involved in the regulation of the actin cytoskeleton (Blader, 1999) and *SLT2* in cell wall integrity (Mazzoni, 1993). *BEM2* encodes a GTPase-activating protein required for bud emergence which involves the polarization of actin cables to the site of bud growth (Peterson, 1994, Kim, 1994). *SAC6* encodes the protein fimbrin which is involved in actin cross-linking and is important for the development and maintenance of cell polarity (Adams, 1991). *GCS1* encodes a GTPase-activating protein for Arf1p which is required for vesicle budding through the interaction of cytoplasmic coat proteins with intracellular organelles (Poon, 1996). *SLT2* is a mitogen-activated protein (MAP) kinase which provides a compensation mechanism to cells undergoing cell wall related stress (de Nobel, 2000). Genetic interactions indicate that when the cell structure genes, *SLT2* and *BEM2*, are deleted, both have negative effects on *ERG11*. This emphasizes the importance of maintaining cell wall/cytoskeletal and membrane integrity simultaneously.

3.2 Complementation assay

To exclude the possibility that potential secondary mutations that may be present in the deletion strains were responsible for the fungicidal phenotype, we complemented the FCZ-fungicidal strains with plasmid-born copies of their respective deleted genes (Gelperin, 2005). The presence of the over-expressed gene enabled the transformants to survive lethal

concentrations of FCZ. However, over-expression of the FCZ-fungicidal genes in the wild type strain did not confer resistance beyond levels tested for the wild type.

3.3 Microarray analysis

3.3.1 Microarray analysis of the FCZ-fungicidal genes

Microarray analysis was performed on the twenty-three FCZ-fungicidal deletion strains compared to the wild type strain. Dye swap microarray analyses, which involved reversing RNA samples labelled with either cyanine 3- or cyanine 5- dCTP dye, were performed on different days. Genetic profiles for each of the deletion strains were compared and clustered on a dendogram (Figure 4). An agglomerative clustering method was used which adds edges individually, merging the two closest clusters at each step. The measure of closeness was computed with Ward's method which merges candidate clusters that are closest together (Ward, 1963). Approximately Unbiased (AU) p-value and Bootstrap Probability (BP) p-value were used to compute the statistical significance of the clustering. A p-value of 0.01 provides 99% statistical significance, thus the more elevated the value, the more significant the cluster.

As would be expected, the expression profiles for dye swapped deletion strains clustered together. Additionally, deletion strains compromised in similar functions gave comparable transcriptional profiles, for example the V-ATPase class of deletion strains clustered together on the dendogram.

3.3.2 Microarray analysis of Δ *pdr5* deletion strain treated with FCZ

In an attempt to determine commonly affected genes or pathways among the FCZ-fungicidal genes and FCZ treatment of cells, microarray analysis was also performed on deletion strain Δ*pdr5* treated with fluconazole compared to the untreated wild type strain. The Δ*pdr5* deletion was used instead of the wild type strain because smaller quantities of FCZ

Figure 4. Clustering of transcriptional profiles generated from the FCZ-fungicidal strains.

The dendogram correlating the transcriptional profiles of the FCZ-fungicidal strains, demonstrates that the profiles which cluster together belong to deletion stains of the same functional class. **I** Δ*ssn3*, Δ*med2* and Δ*srb8* belong to the mediator complex. **II** Δ*spt20*, Δ*ngg1*, Δ*ada2*, Δ*gcn5* belong to the SAGA complex. **III** Δ*tfp1*, Δ*vma4*, Δ*vma10*, Δ*vma13*, Δ*vma22*, Δ*vph2* belong to the V-ATPase complex. **IV** Δ*bem2*, Δ*gcs1*, Δ*sac6*, Δ*slt2* belong to the cytoskeletal class.

Approximately Unbiased (AU) p-value and Bootstrap Probability (BP) p-value were used to compute the statistical significance of the clustering. The higher the value, the more significant the cluster is. The edge # indicates the order in which the edges/branch points were formed.

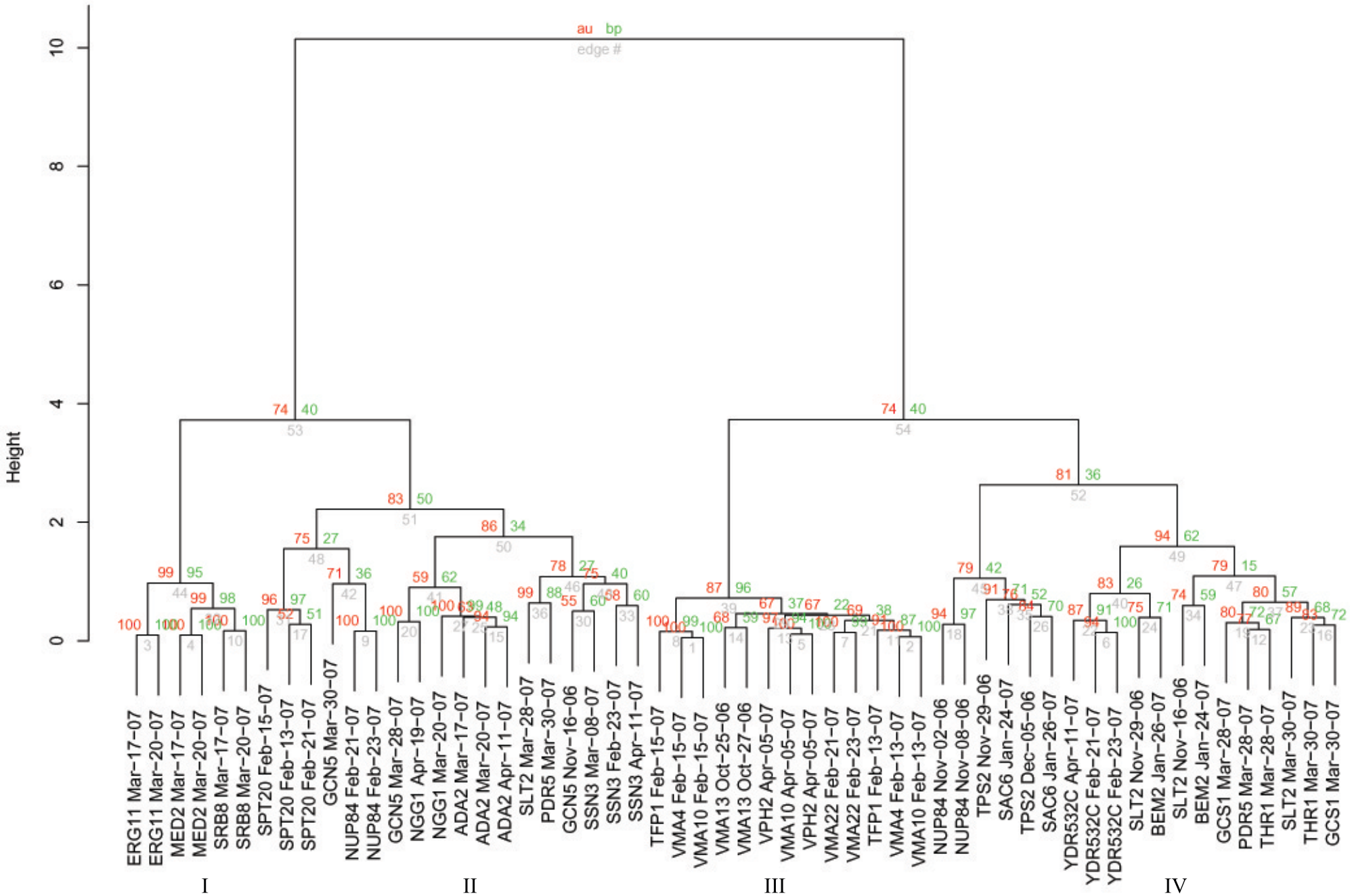
au bp
edge #
Height
0
2
4
6
8
10
ERG11 Mar−17−07
ERG11 Mar−20−07
MED2 Mar−17−07
MED2 Mar−20−07
SRB8 Mar−17−07
SRB8 Mar−20−07
SPT20 Feb−15−07
SPT20 Feb−13−07
SPT20 Feb−21−07
GCN5 Mar−30−07
NUP84 Feb−21−07
NUP84 Feb−23−07
GCN5 Mar−28−07
NGG1 Apr−19−07
NGG1 Mar−20−07
ADA2 Mar−17−07
ADA2 Mar−20−07
ADA2 Apr−11−07
SLT2 Mar−28−07
PDR5 Mar−30−07
GCN5 Nov−16−06
SSN3 Mar−08−07
SSN3 Feb−23−07
SSN3 Apr−11−07
TFP1 Feb−15−07
VMA4 Feb−15−07
VMA10 Feb−15−07
VMA13 Oct−25−06
VMA13 Oct−27−06
VPH2 Apr−05−07
VMA10 Apr−05−07
VPH2 Apr−05−07
VMA22 Feb−21−07
VMA22 Feb−23−07
TFP1 Feb−13−07
VMA4 Feb−13−07
VMA10 Feb−13−07
NUP84 Nov−02−06
NUP84 Nov−08−06
TPS2 Nov−29−06
SAC6 Jan−24−07
TPS2 Dec−05−06
SAC6 Jan−26−07
YDR532C Apr−11−07
YDR532C Feb−21−07
YDR532C Feb−23−07
SLT2 Nov−29−06
BEM2 Jan−26−07
SLT2 Nov−16−06
BEM2 Jan−24−07
GCS1 Mar−28−07
PDR5 Mar−28−07
THR1 Mar−28−07
SLT2 Mar−30−07
THR1 Mar−30−07
GCS1 Mar−30−07
I
II
III
IV

could be used on the drug-pump deficient Δ*pdr5* strain. Such large quantities of FCZ were required to treat wild type cells for microarray analysis that the transcriptional profile obtained could be skewed due to additional stresses such as elevated salt concentrations. As would be expected, since FCZ targets the ergosterol biosynthesis pathway, most genes involved in ergosterol biosynthesis were up-regulated in the strain treated with FCZ (Table 4). These genes have been previously reported to be significantly up-regulated when treated with azole antifungal agents (Bammert, 2000).

Using the expression profiles obtained, a signature heatmap of the cell responses to FCZ treatment and the FCZ-fungicidal deletion strains was generated (Figure 5). The expression profiles for each of the FCZ-fungicidal deletion strains and the FCZ-treatment were compared according to significantly differentially expressed over-represented gene-ontology (GO) categories (from www.geneontology.org). The most significantly differentially expressed categories belonged to ion transport, amino acid biosynthesis/metabolism, ATP synthesis coupled electron transport, and sterol/ergosterol biosynthesis/metabolism. In acquiring a better understanding of the cells' responses, information on which processes were over- and under-expressed was required.

Upon specific analysis of the over-represented up-regulated categories, amino acid biosynthesis/ metabolism, ergosterol/sterol biosynthesis/metabolism, and ion transport/homeostasis were determined to be the most significant (Figure 6). The over-expression of categories involved in amino acid biosynthesis and metabolism is observed across almost all FCZ-fungicidal deletion strains and both FCZ treatment profiles. The up-regulation of these categories is suggested to be accounted for by stresses related to nitrogen limitations. The correct response to nitrogen sources, which are essential for cell survival, might not arise in FCZ-fungicidal strains and cells undergoing FCZ treatment.

Table 4 Genes involved in the ergosterol biosynthesis pathway which were up-regulated upon treatment with FCZ for 180 minutes
Gene descriptions from www.yeastgenome.org.

Gene name	Gene description	Log2Ratio
ERG3	C-5 sterol desaturase, catalyzes the introduction of a C-5(6) double bond into episterol, a precursor in ergosterol biosynthesis; mutants are viable, but cannot grow on non-fermentable carbon sources	3.069266
ERG2	C-8 sterol isomerase, catalyzes the isomerization of the δ-8 double bond to the δ-7 position at an intermediate step in ergosterol biosynthesis	2.225376
ERG11	Lanosterol 14-α-demethylase, catalyzes the C-14 demethylation of lanosterol to form 4,4"-dimethyl cholesta-8,14,24-triene-3-β-ol in the ergosterol biosynthesis pathway; member of the cytochrome P450 family	2.187839
ERG6	Delta(24)-sterol C-methyltransferase, converts zymosterol to fecosterol in the ergosterol biosynthetic pathway by methylating position C-24; localized to both lipid particles and mitochondrial outer membrane	1.995591
ERG26	C-3 sterol dehydrogenase, catalyzes the second of three steps required to remove two C-4 methyl groups from an intermediate in ergosterol biosynthesis	1.859788
ERG1	Squalene epoxidase, catalyzes the epoxidation of squalene to 2,3-oxidosqualene; plays an essential role in the ergosterol-biosynthesis pathway and is the specific target of the antifungal drug terbinafine	1.781756
ERG27	3-keto sterol reductase, catalyzes the last of three steps required to remove two C-4 methyl groups from an intermediate in ergosterol biosynthesis; mutants are sterol auxotrophs	1.412325
ERG28	Endoplasmic reticulum membrane protein, may facilitate protein-protein interactions between the Erg26p dehydrogenase and the Erg27p 3-ketoreductase and/or tether these enzymes to the ER, also interacts with Erg6p	1.283961
ERG9	Farnesyl-diphosphate farnesyl transferase (squalene synthase), joins two farnesyl pyrophosphate moieties to form squalene in the sterol biosynthesis pathway	1.072729

Figure 5. Heatmap of over-represented differentially expressed GO biological categories among FCZ-treated and FCZ-fungicidal strains

Over-represented differentially expressed GO biological categories from the expression profiles generated by the FCZ-fungicidal deletion strains and FCZ treatment of deletion strain Δ*pdr5* are compared on a heatmap. Go categories involved in ion transport, amino acid metabolism/biosynthesis, ATP synthesis coupled electron transport, and ergosterol/sterol biosynthesis are most significantly differentially expressed.


Color Key and Histogram
Count
0
1200
0
4
8
−log10(p−value)
sterol biosynthesis
sterol metabolism
steroid biosynthesis
steroid metabolism
ergosterol metabolism
ergosterol biosynthesis
alcohol metabolism
ribosomal subunit assembly
purine nucleotide metabolism
purine nucleotide biosynthesis
purine ribonucleotide metabolism
purine ribonucleotide biosynthesis
ribonucleotide metabolism
ribonucleotide biosynthesis
nucleotide biosynthesis
nucleotide metabolism
pyridine nucleotide metabolism
NADPH regeneration
protein folding
amino acid metabolism
amino acid and derivative metabolism
amine metabolism
nitrogen compound metabolism
nitrogen compound biosynthesis
amine biosynthesis
amino acid biosynthesis
branched chain family amino acid metabolism
branched chain family amino acid biosynthesis
arginine metabolism
urea cycle intermediate metabolism
glutamine family amino acid biosynthesis
sphingolipid metabolism
nitrogen compound catabolism
amine catabolism
amino acid catabolism
aspartate family amino acid catabolism
aspartate family amino acid metabolism
glutamine family amino acid metabolism
cellular lipid metabolism
lipid metabolism
lipid biosynthesis
hydrogen ion homeostasis
vacuolar acidification
pH reduction
cellular pH reduction
regulation of cellular pH
regulation of pH
monovalent inorganic cation homeostasis
generation of precursor metabolites and energy
energy derivation by oxidation of organic compounds
main pathways of carbohydrate metabolism
cofactor metabolism
manganese ion transport
cellular respiration
aerobic respiration
serine family amino acid metabolism
SRP−dependent cotranslational protein targeting to membrane, translocation
acetyl−CoA catabolism
tricarboxylic acid cycle
coenzyme catabolism
cofactor catabolism
acetyl−CoA metabolism
tricarboxylic acid cycle intermediate metabolism
cellular carbohydrate metabolism
carbohydrate metabolism
coenzyme metabolism
ethanol metabolism
sulfur amino acid metabolism
carbohydrate transport
hexose catabolism
glucose catabolism
glucose metabolism
alcohol catabolism
monosaccharide catabolism
cellular carbohydrate catabolism
carbohydrate catabolism
glycolysis
ion transport
cation transport
transition metal ion transport
di−, tri−valent inorganic cation transport
metal ion transport
siderophore transport
siderophore−iron transport
iron ion transport
ATP synthesis coupled electron transport (sensu Eukaryota)
ATP synthesis coupled electron transport
electron transport
oxidative phosphorylation
mitochondrial electron transport, cytochrome c to oxygen
regulation of translational fidelity
ion homeostasis
cell ion homeostasis
cation homeostasis
homeostasis
cell homeostasis
di−, tri−valent inorganic cation homeostasis
transition metal ion homeostasis
metal ion homeostasis
ATP biosynthesis
nucleoside phosphate metabolism
energy coupled proton transport, down electrochemical gradient
ATP synthesis coupled proton transport
ATP metabolism
purine nucleoside triphosphate biosynthesis
purine nucleoside triphosphate metabolism
purine ribonucleoside triphosphate metabolism
purine ribonucleoside triphosphate biosynthesis
proton transport
hydrogen transport
monovalent inorganic cation transport
ribonucleoside triphosphate biosynthesis
ribonucleoside triphosphate metabolism
nucleoside triphosphate biosynthesis
nucleoside triphosphate metabolism
SSN3
VMA13
VMA22
VPH2
TFP1
VMA10
VMA4
NUP84
GCN5
NGG1
SPT20
MED2
BEM2
YDR532C
ADA2
PDR5.FCZ.180min
SAC6
SLT2
THR1
TPS2
GCS1
SRB8
PDR5
ERG11
PDR5.FCZ.90min

Figure 6. Heatmap of over-represented up-regulated GO biological categories among FCZ-treated and FCZ-fungicidal strains

Over-represented up-regulated GO biological categories are compared on a heatmap for the expression profiles generated by the FCZ-fungicidal deletion strains and FCZ treatment of deletion strain Δ*pdr5*. Categories amino acid metabolism, amino acid and derivative metabolism, amine metabolism, nitrogen compound metabolism, amine biosynthesis, nitrogen compound biosynthesis and amino acid biosynthesis are up-regulated for almost every FCZ-fungicidal strain and both FCZ-treatment profiles. Sterol biosynthesis, steroid biosynthesis, steroid metabolism, sterol metabolism, ergosterol metabolism and ergosterol biosynthesis are highly up-regulated only for FCZ-treatment profiles and the V-ATPase class of FCZ-fungicidal strains. Cellular ion transport and homeostasis categories are highly up-regulated for the V-ATPase class of FCZ-fungicidal strains, especially categories iron transport and iron assimilation.


Color Key and Histogram
Count
0
1500
0
4
8
−log10(pValue)
sterol biosynthetic process
steroid biosynthetic process
steroid metabolic process
sterol metabolic process
ergosterol metabolic process
ergosterol biosynthetic process
monocarboxylic acid metabolic process
coenzyme metabolic process
cofactor metabolic process
NAD metabolic process
nucleotide metabolic process
pyridine nucleotide metabolic process
nicotinamide metabolic process
oxidoreduction coenzyme metabolic process
water−soluble vitamin metabolic process
vitamin metabolic process
carbohydrate metabolic process
cellular carbohydrate metabolic process
glucose import
monosaccharide transport
hexose transport
carbohydrate transport
pentose metabolic process
pentose−phosphate shunt, oxidative branch
monosaccharide catabolic process
alcohol catabolic process
cellular carbohydrate catabolic process
carbohydrate catabolic process
glucose catabolic process
hexose catabolic process
monosaccharide metabolic process
hexose metabolic process
glucose metabolic process
alcohol metabolic process
pyruvate metabolic process
glycolysis
alcohol biosynthetic process
monosaccharide biosynthetic process
hexose biosynthetic process
gluconeogenesis
amino acid metabolic process
amino acid and derivative metabolic process
amine metabolic process
nitrogen compound metabolic process
serine family amino acid metabolic process
amine biosynthetic process
nitrogen compound biosynthetic process
amino acid biosynthetic process
branched chain family amino acid metabolic process
branched chain family amino acid biosynthetic process
aromatic compound metabolic process
aromatic amino acid family metabolic process
protein folding
protein refolding
SRP−dependent cotranslational protein targeting to membrane, translocation
intracellular protein transport across a membrane
glutamine family amino acid biosynthetic process
arginine biosynthetic process
arginine metabolic process
urea cycle intermediate metabolic process
aspartate family amino acid biosynthetic process
nitrogen compound catabolic process
amine catabolic process
amino acid catabolic process
glutamine family amino acid metabolic process
sphingolipid metabolic process
aspartate family amino acid metabolic process
manganese ion transport
asparagine biosynthetic process
sulfur amino acid metabolic process
methionine metabolic process
monovalent inorganic cation transport
sodium ion transport
lipid biosynthetic process
lipid metabolic process
cellular lipid metabolic process
nucleobase metabolic process
amino acid derivative biosynthetic process
amino acid derivative metabolic process
iron assimilation by chelation and transport
siderophore−iron transport
iron assimilation
siderophore transport
iron ion transport
di−, tri−valent inorganic cation transport
di−, tri−valent inorganic cation homeostasis
cellular di−, tri−valent inorganic cation homeostasis
vitamin transport
iron ion homeostasis
cellular iron ion homeostasis
cation homeostasis
cellular cation homeostasis
cellular chemical homeostasis
cellular ion homeostasis
ion homeostasis
chemical homeostasis
homeostatic process
cellular homeostasis
regulation of biological quality
zinc ion homeostasis
cellular zinc ion homeostasis
response to metal ion
threonine metabolic process
vacuolar protein catabolic process
ion transport
cation transport
metal ion transport
transition metal ion transport
serine family amino acid catabolic process
carboxylic acid transport
organic acid transport
amino acid transport
amine transport
NADPH regeneration
NADP metabolic process
pentose−phosphate shunt
glutamate metabolic process
transposition, RNA−mediated
transposition
NUP84
ADA2
NGG1
SPT20
YDR532C
PDR5.FCZ.180min
PDR5.FCZ.90min
SLT2
THR1
BEM2
TPS2
MED2
SAC6
ERG11
PDR5
SRB8
SSN3
GCN5
GCS1
VPH2
VMA22
VMA13
VMA4
TFP1
VMA10

The ergosterol/sterol biosynthesis/metabolism categories were highly up-regulated for the FCZ treatment profiles, as expected, because FCZ targets the ergosterol pathway. However, the V-ATPase class of FCZ-fungicidal strains also exhibited significant up-regulation in these categories. These observations suggest a link between *vma* mutants and the over-expression of the ergosterol pathway.

Ion transport and homeostasis is another category which was significantly up-regulated across the V-ATPase mutants. Upon further analysis, over-expression of genes specifically involved in iron metabolism, cellular iron ion homeostasis, iron ion transport, and siderophore transport were restricted to all *vma* mutants among the FCZ-fungicidal deletion strains (Figure 7). It has been previously reported that genes involved in iron transport and homeostasis are over-expressed in V-ATPase mutants (Milgrom, 2007).

Investigation into specific over-represented down-regulated categories showed a significant response across the *vma* mutants corresponding to the classes involving organelle ATP synthesis coupled electron transport, ATP synthesis coupled electron transport, electron transport, and oxidative phosphorylation (Figure 8). It is suggested that impaired iron uptake in *vma* mutants could be responsible for the down-regulation observed by causing a deficiency in Fe-S clusters in the electron transport chain. Although over-represented down-regulated categories from the FCZ treatment profiles do not correlate with those from the FCZ-fungicidal gene profiles, deletion strains from the same classes do produce similar down-regulation patterns. For example, Δ*srb8* and Δ*ssn3* display similar expression profiles as well as Δ*slt2*, Δ*bem2*, and Δ*gcs1* and the Δ*vma*s have resembling down-regulated genes GO categories.

3.4 Reporter genes

From the FCZ-fungicidal transcriptional profiles, candidate genes to be used in

Figure 7. Heatmap of significantly up-regulated iron related genes

GO biological annotated categories representing iron metabolism, cellular iron ion homeostasis, iron ion transport and siderophore transport are significantly up-regulated only in the V-ATPase mutant strains.

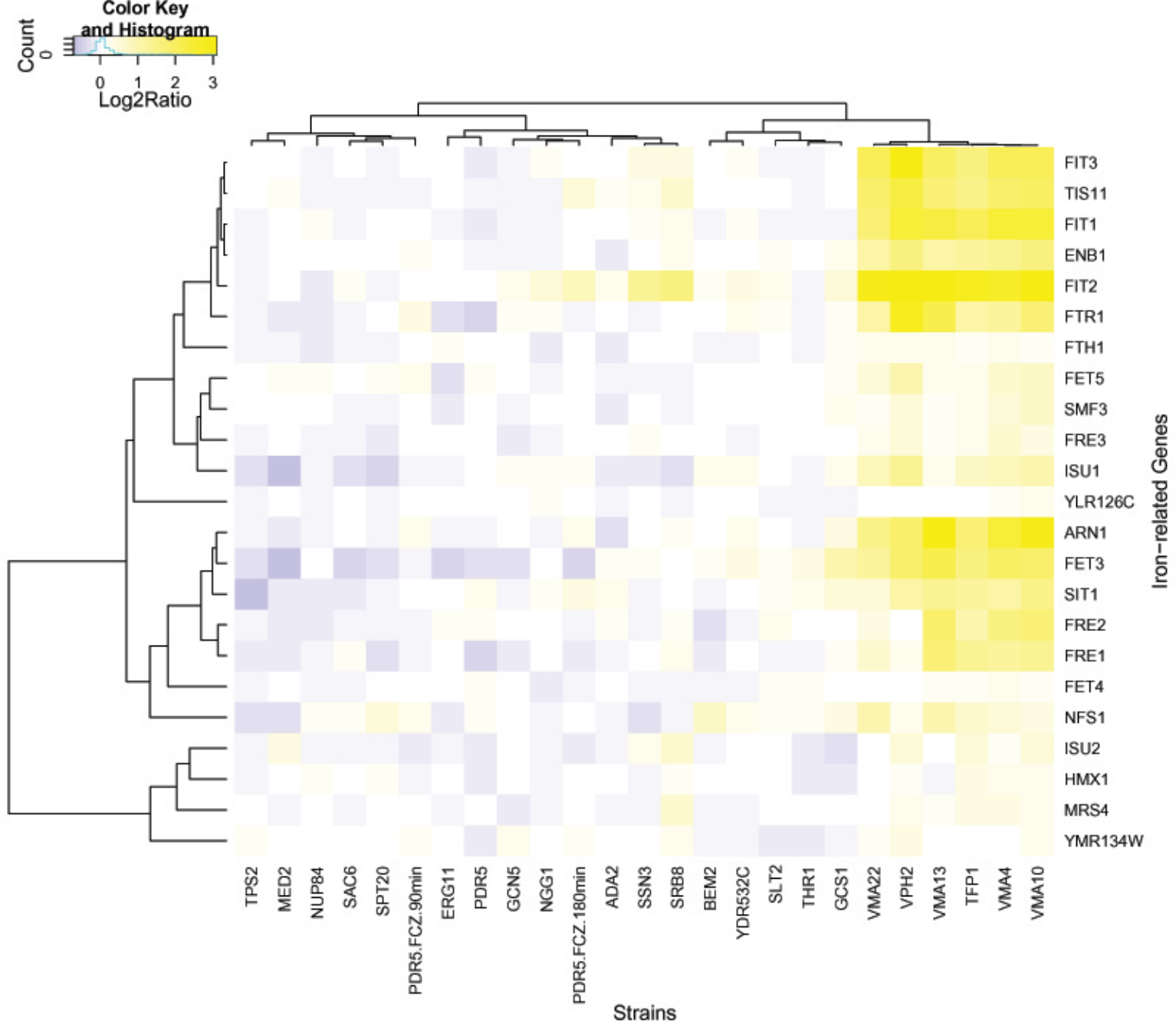
Color Key and Histogram
Count
0
0
1
2
3
Log2Ratio
FIT3
TIS11
FIT1
ENB1
FIT2
FTR1
FTH1
FET5
SMF3
FRE3
ISU1
YLR126C
ARN1
FET3
SIT1
FRE2
FRE1
FET4
NFS1
ISU2
HMX1
MRS4
YMR134W
Iron−related Genes
TPS2
MED2
NUP84
SAC6
SPT20
PDR5.FCZ.90min
ERG11
PDR5
GCN5
NGG1
PDR5.FCZ.180min
ADA2
SSN3
SRB8
BEM2
YDR532C
SLT2
THR1
GCS1
VMA22
VPH2
VMA13
TFP1
VMA4
VMA10
Strains

Figure 8. Heatmap of over-represented down-regulated GO biological categories among FCZ-treated and FCZ-fungicidal strains

Over-represented down-regulated GO biological categories are compared on a heatmap for the expression profiles generated by the FCZ-fungicidal deletion strains and FCZ treatment of deletion strain Δ*pdr5*. Categories organelle ATP synthesis coupled electron transport, ATP synthesis coupled electron transport, electron transport, and oxidative phosphorylation are greatly down-regulated in the V-ATPase class of FCZ-fungicidal strains. There is common down-regulation among the same FCZ-fungicidal gene classes. Δ*srb8* and Δ*ssn3* display similar expression profiles as well as Δ*slt2*, Δ*bem2*, and Δ*gcs1* and the Δ*vma*s have resembling down-regulated GO categories.

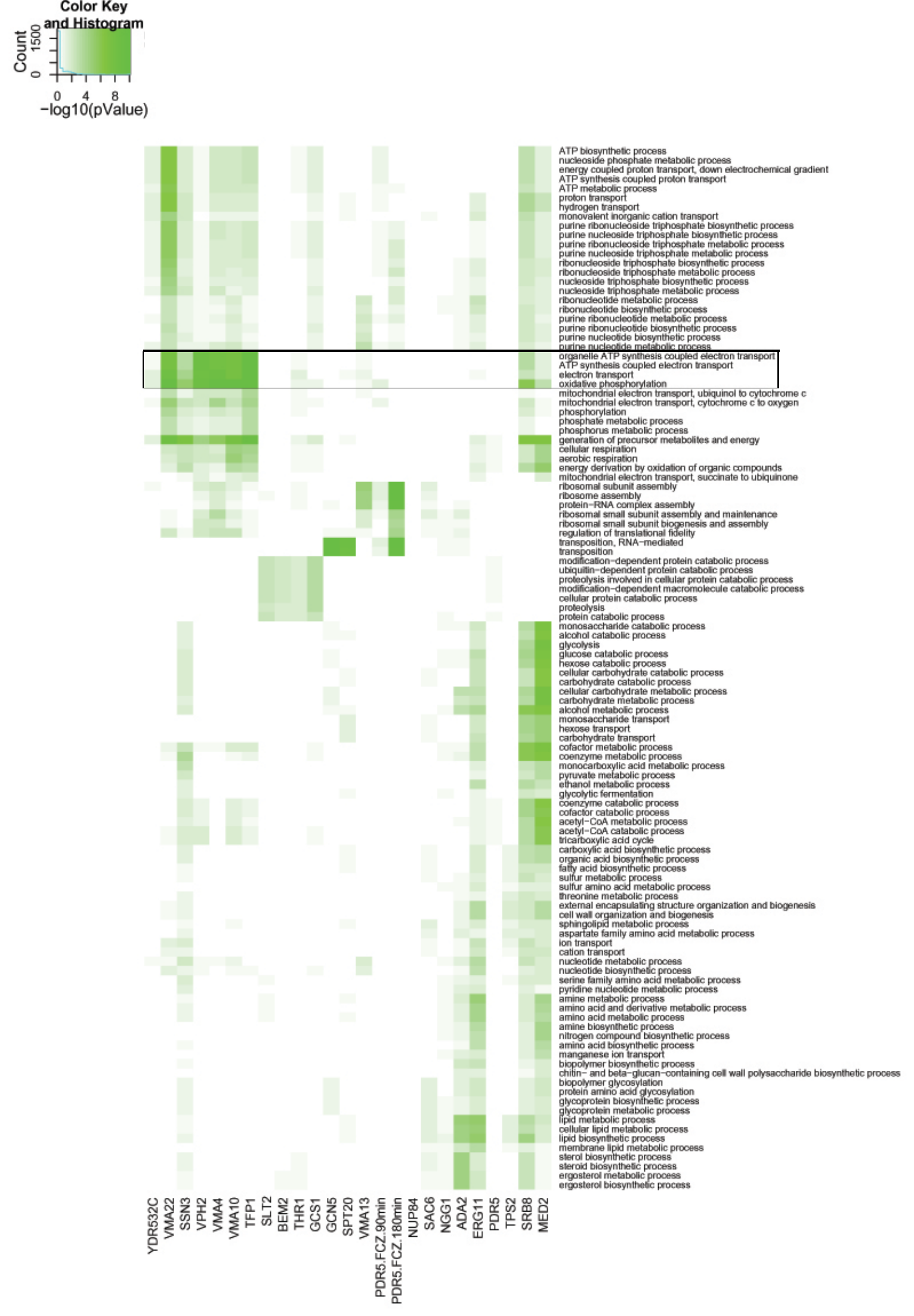
Color Key and Histogram
Count
0
1500
0
4
8
−log10(pValue)
ATP biosynthetic process
nucleoside phosphate metabolic process
energy coupled proton transport, down electrochemical gradient
ATP synthesis coupled proton transport
ATP metabolic process
proton transport
hydrogen transport
monovalent inorganic cation transport
purine ribonucleoside triphosphate biosynthetic process
purine nucleoside triphosphate biosynthetic process
purine ribonucleoside triphosphate metabolic process
purine nucleoside triphosphate metabolic process
ribonucleoside triphosphate biosynthetic process
ribonucleoside triphosphate metabolic process
nucleoside triphosphate biosynthetic process
nucleoside triphosphate metabolic process
ribonucleotide metabolic process
ribonucleotide biosynthetic process
purine ribonucleotide metabolic process
purine ribonucleotide biosynthetic process
purine nucleotide biosynthetic process
purine nucleotide metabolic process
organelle ATP synthesis coupled electron transport
ATP synthesis coupled electron transport
electron transport
oxidative phosphorylation
mitochondrial electron transport, ubiquinol to cytochrome c
mitochondrial electron transport, cytochrome c to oxygen
phosphorylation
phosphate metabolic process
phosphorus metabolic process
generation of precursor metabolites and energy
cellular respiration
aerobic respiration
energy derivation by oxidation of organic compounds
mitochondrial electron transport, succinate to ubiquinone
ribosomal subunit assembly
ribosome assembly
protein−RNA complex assembly
ribosomal small subunit assembly and maintenance
ribosomal small subunit biogenesis and assembly
regulation of translational fidelity
transposition, RNA−mediated
transposition
modification−dependent protein catabolic process
ubiquitin−dependent protein catabolic process
proteolysis involved in cellular protein catabolic process
modification−dependent macromolecule catabolic process
cellular protein catabolic process
proteolysis
protein catabolic process
monosaccharide catabolic process
alcohol catabolic process
glycolysis
glucose catabolic process
hexose catabolic process
cellular carbohydrate catabolic process
carbohydrate catabolic process
cellular carbohydrate metabolic process
carbohydrate metabolic process
alcohol metabolic process
monosaccharide transport
hexose transport
carbohydrate transport
cofactor metabolic process
coenzyme metabolic process
monocarboxylic acid metabolic process
pyruvate metabolic process
ethanol metabolic process
glycolytic fermentation
coenzyme catabolic process
cofactor catabolic process
acetyl−CoA metabolic process
acetyl−CoA catabolic process
tricarboxylic acid cycle
carboxylic acid biosynthetic process
organic acid biosynthetic process
fatty acid biosynthetic process
sulfur metabolic process
sulfur amino acid metabolic process
threonine metabolic process
external encapsulating structure organization and biogenesis
cell wall organization and biogenesis
sphingolipid metabolic process
aspartate family amino acid metabolic process
ion transport
cation transport
nucleotide metabolic process
nucleotide biosynthetic process
serine family amino acid metabolic process
pyridine nucleotide metabolic process
amine metabolic process
amino acid and derivative metabolic process
amino acid metabolic process
amine biosynthetic process
nitrogen compound biosynthetic process
amino acid biosynthetic process
manganese ion transport
biopolymer biosynthetic process
chitin− and beta−glucan−containing cell wall polysaccharide biosynthetic process
biopolymer glycosylation
protein amino acid glycosylation
glycoprotein biosynthetic process
glycoprotein metabolic process
lipid metabolic process
cellular lipid metabolic process
lipid biosynthetic process
membrane lipid metabolic process
sterol biosynthetic process
steroid biosynthetic process
ergosterol metabolic process
ergosterol biosynthetic process
YDR532C
VMA22
SSN3
VPH2
VMA4
VMA10
TFP1
SLT2
BEM2
THR1
GCS1
GCN5
SPT20
VMA13
PDR5.FCZ.90min
PDR5.FCZ.180min
NUP84
SAC6
NGG1
ADA2
ERG11
PDR5
TPS2
SRB8
MED2

constructing a growth reporter were selected for being highly up-regulated in the deletion strains but not over-expressed in the wild type strain (Figure 9). According to our chemical genetics approach, the reporter is required to be activated in the absence of one of the FCZ-fungicidal genes. Thus, from the microarray data, the relevant genes would be the ones most highly up-regulated. Because the reporter assay is performed in the wild type background, the gene should not be over-expressed in the wild type strain. According to Figure 9, the genes which were most highly expressed were *FIT2* and *FIT3*; this up-regulation occurred across all the deletion strains belonging to the V-ATPase complex. The *FIT2* and *FIT3* gene products are both mannoproteins that are incorporated into the cell wall via a glycosylphosphatidylinositol (GPI) anchor. They are involved in the retention of siderophore-iron in the cell wall (www.yeastgenome.org). Additionally, gene *YLR162W* was strongly over-expressed in genes Δ*vph2*, Δ*gcs1* and Δ*thr1*.

Using bioinformatics tools to predict which significantly up-regulated genes would generate good reporters for the assay, two different assessments were made based on the expression of these genes in other yeast expression profiles (Tables 5 and 6). Table 5 summarizes the assessment of candidate reporters based on the up- or down- fold change alone whereas the assessment made in Table 6 also incorporates the differential expression p-values. From this prediction and Figure 9, three reporter genes were chosen to investigate in fungicidal strains is presented in Table 7. The *FIT2* gene was predicted to generate the best reporter according to the assessment made in Table 5 whereas and *CIT2* was predicted to produce an ideal reporter according to the assessment provided in Table 6. Because both these genes were up-regulated in the same deletion strains (Δ*vma*s), *YLR162W* was chosen because it was significantly up-regulated in different deletion strains (Δ*gcs1*, Δ*thr1*, andΔ*vph2*). The purpose of this reporter assay is to identify drugs which act fungicidal synergistically with FCZ and to simultaneously identify their targets. The drug targets should

Figure 9. Heatmap of significantly up-regulated genes from FCZ-fungicidal profiles

A heatmap was generated to identify genes which were highly up-regulated among the FCZ-fungicidal strains but not in the wild type strain. Significantly over-expressed genes in several FCZ-fungicidal strains were chosen to be used in the construction of the reporter. Genes *FIT2* and *FIT3* are shown to be the most highly up-regulated genes.

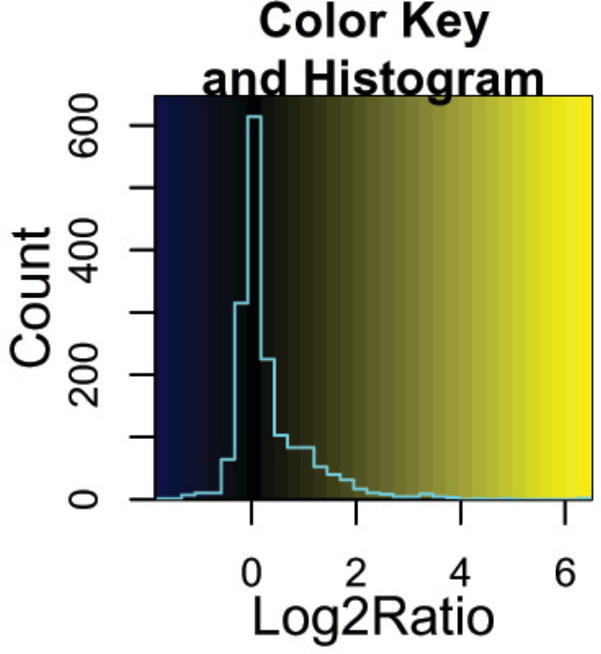
Color Key
and Histogram
Count
0
200
400
600
0
2
4
6
Log2Ratio


transport
amino acid and derivative metabolism
RNA metabolism
sporulation
cell homeostasis
protein modification
organelle organization and biogenesis
lipid metabolism
cell wall organization and biogenesis
electron transport
carbohydrate metabolism
vitamin metabolism
cytoskeleton organization and biogenesis
biological process unknown

FIT1
TIS11
ENB1
ERG27
YDR476C
ARN2
ARN1
FET3
TPN1
SIT1
FRE1
VHT1
FRE2
PRB1
YNL134C
YLR194C
YPS1
HXT5
ISU1
HXT2
YAL068C
YGL039W
SPS100
DAN3
NCA3
TIR3
FIT2
FTR1
FIT3
COT1
SPI1
SNZ1
PAU4
YFL066C
YHL050C
YHR214W-A
YHR214W
BAT2
STB3
NCP1
BAP3
CAR1
CIT2
YBL112C
RCR1
ARE1
YCR102C
YEL074W
MOH1
HXT12
ARO10
TRP5
HIP1
FCY2
DED1
ADE5,7
YCL049C
YCL045C
ABP1
PRD1
ARG1
CPA1
SBA1
YKR047W
YFL064C
YPR202W
YER189W
YLR462W
YHL049C
PPQ1
NCE102
YLR162W
IDP2
SKI2
ERG11
NGG1
ADA2
GCN5
MED2
SRB8
SPT20
TPS2
SAC6
NUP84
BEM2
YDR532C
SLT2
PDR5
THR1
GCS1
SSN3
VPH2
VMA22
TFP1
VMA13
VMA10
VMA4
Deletion Strain

Table 5. Bioinformatics analysis on the predictive ability of potential reporters.
Based only on fold change (<=0.5 or >=2) in other yeast expression profiles, the candidate reporter genes were ranked based on their ability to report on the under-expression of their target FCZ-fungicidal genes. The candidate reporter gene with the most potential is considered to be the one with the lowest false positive rate.

Gene	True Positive Rate	False Negative Rate	False Positive Rate
FIT2	0.3865	0.6135	0.1795
FET3	0.2736	0.7264	0.1929
TIS11	0.3238	0.6762	0.2517
ARN1	0.3926	0.6074	0.2634
YFL064C	0.2500	0.7500	0.2705
YNL134C	0.3639	0.6361	0.2722
FIT1	0.2006	0.7994	0.3000
FIT3	0.5100	0.4900	0.3232
YDR476C	0.3954	0.6046	0.3268
ENB1	0.2722	0.7278	0.3403
ARN2	0.3066	0.6934	0.3436
YER189W	0.2701	0.7299	0.3588
CIT2	0.2809	0.7191	0.3631
FTR1	0.2751	0.7249	0.3642
YLR194C	0.5067	0.4933	0.4131
SIT1	0.3460	0.6540	0.4220
IDP2	0.3992	0.6008	0.4541
FRE1	0.3012	0.6988	0.4565
HXT2	0.4459	0.5541	0.4607
YLR162W	0.1395	0.8605	0.4615
NCP1	0.1983	0.8017	0.4719
YCL045C	0.1632	0.8368	0.4800
BAT2	0.2691	0.7309	0.5000
SPS100	0.4892	0.5108	0.5022
ABP1	0.2762	0.7238	0.5075
YHL049C	0.1886	0.8114	0.5182
YCL049C	0.4937	0.5063	0.5317
MOH1	0.5071	0.4929	0.5504
FRE2	0.3133	0.6867	0.5517
YBL112C	0.3285	0.6715	0.5584
ARG1	0.3937	0.6063	0.5606
YPR202W	0.1777	0.8223	0.5825
VHT1	0.3388	0.6612	0.5867
ADE5,7	0.2538	0.7462	0.5868
YCR102C	0.2077	0.7923	0.5905
CPA1	0.4335	0.5665	0.5976
DED1	0.2486	0.7514	0.6068
RCR1	0.5362	0.4638	0.6092
YHR214W-A	0.3188	0.6812	0.6118
YHR214W	0.1449	0.8551	0.6154
PFK2	0.3213	0.6787	0.6223
HIP1	0.3279	0.6721	0.6319
YHL050C	0.3684	0.6316	0.6667
YAL068C	0.3902	0.6098	0.6701
ERG2	0.1677	0.8323	0.6747
HXT5	0.6051	0.3949	0.6758
YGL039W	0.2195	0.7805	0.7097
ISU1	0.5478	0.4522	0.7143
NPL3	0.2056	0.7944	0.7284
HIS3	0.3590	0.6410	0.7308

Table 6. Bioinformatics analysis on the predictive ability of potential reporters.

Based on statistically significant (adjusted $p < 0.05$) fold change (<=0.5 or >=2) in other yeast expression profiles, the candidate reporter genes were ranked based on their ability to report on the under-expression of their target FCZ-fungicidal genes. The candidate reporter gene with the most potential here is determined to be the one with the lowest false positive rate. (This Table excludes candidates with false positive rate=1.)

Gene	True Positive Rate	False Negative Rate	False Positive Rate
CIT2	0.5000	0.5000	0.0000
YFL064C	0.7500	0.2500	0.0000
YHL049C	0.3333	0.6667	0.0000
YPR202W	0.3333	0.6667	0.0000
HXT5	1.0000	0.0000	0.6000
YCR102C	1.0000	0.0000	0.6000
YNL134C	0.5000	0.5000	0.6667
SPS100	1.0000	0.0000	0.7143
HXT2	0.5000	0.5000	0.7500
MOH1	1.0000	0.0000	0.7500
FRE1	0.5000	0.5000	0.8000
ARG1	0.5000	0.5000	0.8000
BAT2	0.5000	0.5000	0.8000
YDR476C	0.5000	0.5000	0.8571
YGL039W	1.0000	0.0000	0.8571
HIS3	0.5000	0.5000	0.8571
FIT2	1.0000	0.0000	0.8750
FIT1	0.5000	0.5000	0.8750
CPA1	0.5000	0.5000	0.8750
ARN2	0.5000	0.5000	0.8889
FRE2	0.5000	0.5000	0.8889
RCR1	0.5000	0.5000	0.8889
TIS11	0.5000	0.5000	0.9000
ENB1	0.5000	0.5000	0.9091
ARN1	0.5000	0.5000	0.9167
SIT1	0.5000	0.5000	0.9231
YLR194C	0.5000	0.5000	0.9545
IDP2	0.0000	1.0000	NA
MF(ALPHA)2	0.0000	1.0000	NA
PFK2	0.0000	1.0000	NA
SKI2	0.0000	1.0000	NA
YCL045C	NA	NA	NA
YHR214W	0.0000	1.0000	NA
YHR214W-A	0.0000	1.0000	NA
YLR162W	0.0000	1.0000	NA

Table 7. Fold change of genes *FIT2*, *CIT2*, and *YLR162W* across the FCZ-fungicidal strains.
The greatest fold changes are in **bold.**

FCZ-Fungicidal strain	FIT2	CIT2	YLR162W
SRB8	3.375602	0.966769	2.070013
MED2	1.01332	1.04319	2.900564
NUP84	0.882939	1.051519	1.038025
TFP1	**8.379477**	**2.262818**	1.094582
GCS1	1.51305	1.051094	**9.209666**
TPS2	0.983137	1.186229	1.085004
SAC6	1.116535	1.796529	0.972925
NGG1	1.414613	1.047252	0.834259
ADA2	1.219081	1.015106	2.13901
YDR532C	1.35508	1.521246	1.231116
BEM2	1.146382	0.872307	1.042164
GCN5	1.162334	0.913855	0.763585
ERG11	1.006216	1.096697	1.242596
THR1	0.955872	1.215045	**9.063818**
SLT2	1.158264	1.071319	1.320651
VMA10	**10.00408**	**2.054918**	1.146002
VMA22	**9.052937**	**3.373505**	0.999803
VPH2	**51.55746**	1.15797	**17.12852**
SPT20	0.945183	**4.064419**	1.089309
PDR5	1.056221	1.153077	0.706376
VMA4	**8.544989**	**2.404777**	1.074789
SSN3	2.206908	1.036772	0.988928
VMA13	**13.95263**	**3.125769**	1.033988

involve the FCZ-fungicidal genes whose absence causes up-regulation of the reporter. Thus, it was thought that by generating reporters using the promoters of genes which were up-regulated in different FCZ-fungicidal deletion strains, a more diverse population of compounds could be identified as acting fungicidal synergistically with FCZ. However, although the three genes were predicted to generate ideal reporter genes, only *FIT2* responded as expected. Consequently, the focus of the next sections will be on the *FIT2* reporter.

The reporter was constructed using the promoter of the *FIT2* gene to promote transcription of the *HIS3* gene. The *GAL1* promoter in plasmid pGREG506-HIS3 was replaced with *FIT2*'s promoter through *in vivo* recombination (Figure 10). *In vivo* recombination involved taking the digested pGREG506-HIS3 plasmid, and the PCR product of the *FIT2* promoter with flanking ends homologous to the pGREG506-HIS3 plasmid and transforming them into the Δ*vma4* deletion strain. Thus the reporter is constructed and in one step transformed in the deletion strain Δ*vma4* where its phenotype is to be tested. The advantage of this method over a standard cloning approach is that it is rapid and the phenotype can be assessed immediately.

The rationale underlying this reporter assay is that in the absence of the *VMA* genes, the *FIT2* gene is up-regulated and its promoter will allow for the production of the *HIS3* gene product and growth in media lacking histidine. The *FIT2* reporter behaved as expected: when the construct was transformed into the haploid Δ*vma* deletion strains, growth on media lacking histidine and containing 3-AT was observed (Figure 11A). Because 3-AT is a competitive inhibitor to histidine, only cells with an induced reporter which synthesize their own histidine are able to grow. In contrast, when the reporter gene was transformed into deletion strains Δ*gcs1* and Δ*tps2* which, according to the microarray data, do not over- express the *FIT2* gene, no growth on 3-AT media was observed. When the Δ*vma* haploid deletion strains containing the *FIT2* reporter were mated to the wild type BY4742 *MATα*

Figure 10. Generation of *FIT2* reporter from pGREG506-HIS3

The plasmid pGREG506-HIS3 is digested with restriction enzymes *Asc*1 and *Spe*1, excising the *GAL1* promoter to allow for more efficient *in vivo* recombination. Then, the PCR product corresponding to the *FIT2* promoter with flanking ends homologous to the digested plasmid is transformed into the Δ*vma4* deletion strain along with the digested plasmid; allowing for *in vivo* recombination and producing the *FIT2* reporter.

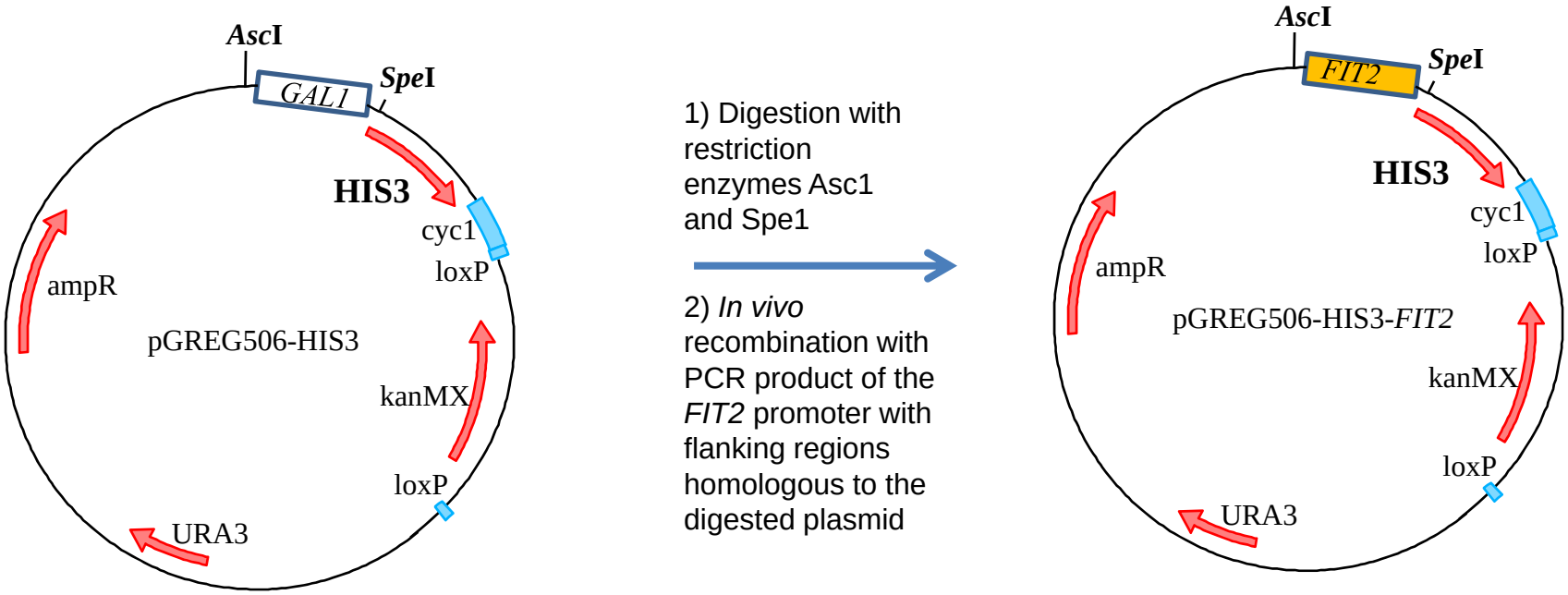
AscI
GAL1
SpeI
HIS3
cyc1
loxP
ampR
pGREG506-HIS3
kanMX
loxP
URA3
1) Digestion with restriction enzymes Asc1 and Spe1
2) In vivo recombination with PCR product of the FIT2 promoter with flanking regions homologous to the digested plasmid
AscI
FIT2
SpeI
HIS3
cyc1
loxP
ampR
pGREG506-HIS3-FIT2
kanMX
loxP
URA3

strain, the diploid strains were unable to grow on media containing 3-AT. By generating the heterozygous diploid strain, one copy of the *VMA* gene is present, inactivating the promoter and preventing the production of the *HIS3* enzyme. To verify that the phenotype of the reporter gene was not haploid specific, the *FIT2* reporter was transformed into the homozygous diploid Δ*vma22* deletion strain and growth was observed on media containing 3-AT. This result indicates that it is not the diploid state which prevents the activation of the reporter but the presence of the *VMA* gene (Figure 11B).

The *FIT2* gene is up-regulated in iron limiting conditions. A previously reported study on the role of iron and FCZ used the iron-chelator apotransferrin to create an iron-deficient environment (Grover, 1996). Using this concept, the *FIT2* reporter in the wild type strain was inoculated in his^- media with 15mM 3-AT in the presence and absence of apotransferrin (6mg/mL) to verify if the reporter would be induced. Growth curves for each were generated: in the absence of apotransferrin, growth was very minimal reaching an OD_{600} value of 0.03 after 46 hours of incubation, however, in the presence of apotransferrin the cells reached an OD_{600} value of 0.8 after the same incubation period. The apotransferrin assay shows that the *FIT2* reporter assay is able to detect changes in the cell and allow for specific growth. This supports our theory that if a compound inactivates one of the *VMA* genes or proteins the reporter should detect it and be activated.

3.5 Sigma LOPAC Screen

The *FIT2* reporter in the wild type strain was used to screen the entire Sigma LOPAC (Library Of Pharmacologically Active Compounds) library which contains 1280 chemically diverse compounds. The *FIT2* reporter is somewhat sensitive to DMSO as concentrations >0.05% up-regulate the reporter. Since the Sigma LOPAC library is dissolved in DMSO and the concentration of the stock plate is 2mM, 1uM was the highest compound concentration

Figure 11. Specificity of *FIT2* reporter construct

A. Assessment of *FIT2* reporter's phenotype

Haploid (H) and heterozygous diploid (D) deletion strains Δ*vma4,* Δ*vma13,* Δ*vma22,* Δ*tps2,* Δ*gcs1,* and wild type strain transformed with the *FIT2* reporter were monitored for growth on his^-, his^- gal, ura^- and his^- media containing 5mM, 10mM and 15mM 3-AT. The control is the wildtype strain transformed with plasmid pGREG 486 which produces the *HIS3* gene product.

B. Verification of *FIT2* reporter's non-haploid specific phenotype

In proving that the *FIT2* reporter's phenotype is not haploid specific, the *FIT2* reporter was transformed in the heterozygous and homozygous diploid Δ*vma22* deletion strains, haploid deletion Δ*vma22* and wildtype strain. Growth was monitored on his^-, his^- gal, ura^- and his^- media containing 5mM, 10mM and 15mM 3-AT.

A.

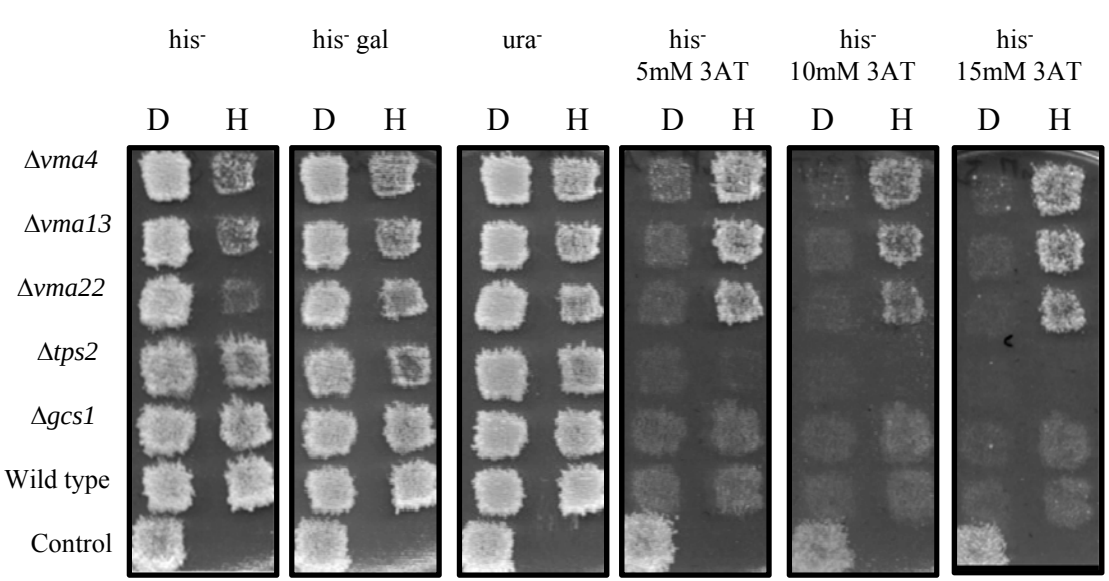
his-
his- gal
ura-
his- 5mM 3AT
his- 10mM 3AT
his- 15mM 3AT
D H D H D H D H D H D H
Δvma4
Δvma13
Δvma22
Δtps2
Δgcs1
Wild type
Control

B.

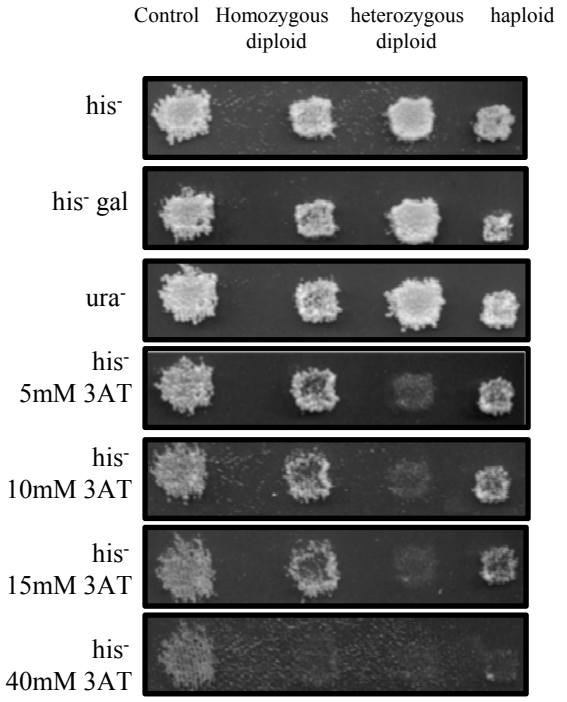
Control
Homozygous diploid
heterozygous diploid
haploid
his-
his- gal
ura-
his- 5mM 3AT
his- 10mM 3AT
his- 15mM 3AT
his- 40mM 3AT

that could be used to treat the cells in this assay.

From this screen, hits were classified according to the database idbs' ActivityBase suite (http://www.idbs.com/ActivityBase/). Given that this is a growth reporter assay, cells will only grow if the reporter is induced by a compound. Thus, by using the untreated controls, hits were determined to be strong if the ratio between the absorbance value at OD_{600} of treated cells over the control cells was equal to or greater than 15. Hits were classified as medium if the ratio was between 10 and 15 and weak if the ratio was between 5 and 10. From the 1280 compounds screened, 67 compounds were classified as hits and added to the cherry-picked plate. This plate was subsequently tested in duplicate with the *FIT2* reporter in the wild type strain. After retesting, one compound could robustly and reproducibly induce the *FIT2* reporter: DPIC (Figure 12).

An additional screen was performed on wild type cells using the entire Sigma LOPAC library and a sub-lethal concentration of FCZ (10μg/mL). This assay was performed to assess the *FIT2* reporter's ability in identifying fluconazole synergistic fungicidal compounds. Upon thorough testing, only DPIC was found to be fungicidal synergistically with fluconazole.

3.6 Diphenyleneiodonium chloride

The purpose of generating this reporter assay was to discover compounds which, in combination with fluconazole, would lead to cell death. In the presence of DPIC (0.3μM) and fluconazole (8μg/mL), *Saccharomyces cerevisiae* cells are unable to grow after incubation for twenty-four hours. After spotting 2μL of these cultures onto a YPD agar plate, cell recovery is observed, however, cell growth is affected. This implies that there is fungistatic synergy between FCZ and DPIC after 24 hours of treatment (Figure 13). Interestingly, when the cells are incubated for longer periods of time (up to eleven days) there is no growth in liquid cultures and when spotted, the number of cells which recover decreases with incubation time

Figure 12. Induction of the *FIT2* reporter by DPIC

A. All the wells shown in this Figure contain the *FIT2* reporter in wild type background in his^- media containing 15mM 3-aminotriazole. Cells were treated with calmidazolium chloride and two different concentrations of DPIC. Additionally, five negative controls were included to demonstrate the lack of growth in the absence of compound. Cells transformed with the *FIT2* reporter only grow in the presence of DPIC. The first panel was taken after 24 hours of incubation, and the second image was taken after an incubation period of 41 hours.

B. Growth curve monitoring OD_{600} absorbance over time. Wild type cells containing the *FIT2* reporter were treated with either: DPIC at two different concentrations (1μM and 5μM), or with positive control apotransferrin (6mg/mL). An untreated control is also represented on the graph. Cells transformed with the *FIT2* reporter display similar growth to the positive control when treated with DPIC, confirming the hit.

C. Chemical structure of DPIC.

A.

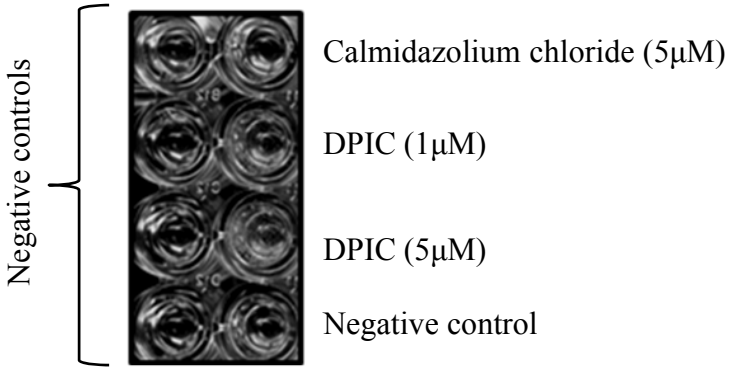

24-hour incubation

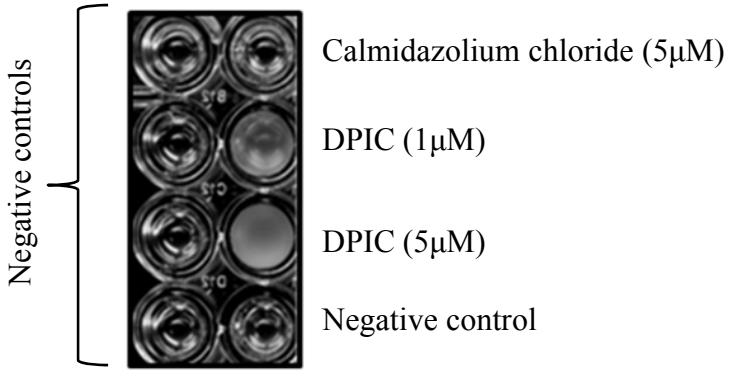

41-hour incubation

B.

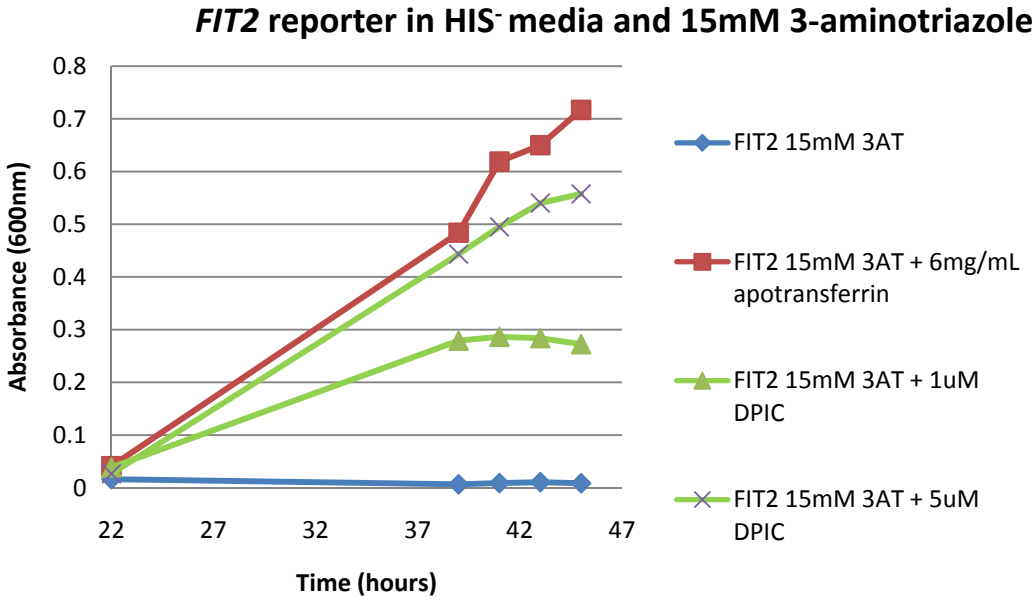

C.

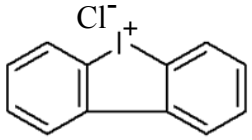

until none recover. This finding suggests that fungicidal synergy occurs between the two compounds over longer incubation periods.

Since *Saccharomyces cerevisiae* is not a pathogenic species, it was of great importance to determine if the *FIT2* reporter's ability to identify FCZ synergistic fungicidal compounds was paralleled in *Candida albicans*. A checkerboard assay performed in *C. albicans* showed similar results to the *Saccharomyces cerevisiae* assay; DPIC synergy with FCZ is observed over time (Figure 13D). The difference between the two species is that higher concentrations of DPIC are required for synergy in *Candida albicans* compared to *Saccharomyces cerevisiae*. Where in *Saccharomyces cerevisiae* 0.3μM of DPIC and 8μg/mL of FCZ prevent cell growth, in *Candida albicans* 80μM of DPIC are required to prevent cell growth with the same concentration of FCZ. It is important to note that in the absence of FCZ, cell growth of either species is not impeded by DPIC, thus this compound alone is not a fungistatic agent to fungal cells.

3.6.1 Diphenyleneiodonium chloride target

The rationale used to generate the novel reporter assay proposes that compounds which activate the reporter target the genes whose deletion causes up-regulation of the reporter. Thus, since the *FIT2* reporter was used to identify DPIC as a synergistic counterpart to FCZ, DPIC is suggested to target a component of the V-ATPase complex. In determining the target of DPIC, the SGA library, containing strains harbouring 3761 single non-essential gene deletions, was screened with sub-lethal concentrations of the compound. Upon retesting on solid and in liquid media, eight deletions strains were determined to be sensitive to DPIC (Table 8a). Interestingly, six of these eight strains not only interact with each other but five of them also interact with at least one of the FCZ-fungicidal genes (Table 8b).

Using a different approach to inquire into V-ATPase components being affected by

Figure 13. Synergy test between DPIC and FCZ in *Saccharomyces cerevisiae* and *Candida albicans*

A. *Saccharomyces cerevisiae* wildtype cells were treated overnight with different concentrations of DPIC and FCZ. A DMSO control experiment was performed in parallel. Cells were spotted on YPD agar media after 24 hours and assessed for growth recovery after two overnight incubations. The image depicted demonstrates initial fungistatic synergy between DPIC and FCZ: although cells recover their growth is affected. **B.** Cells were spotted after five overnight incubations. Fungistatic synergy is detected but fewer cells recover. **C.** Cells were spotted after eleven overnight incubations. Fungicidal synergy occurs between FCZ and DPIC after long incubation periods as no cells are able to recover.

D. This Figure demonstrates DPIC as a synergistic fungicidal counterpart to FCZ in *Candida albicans. Candida albicans* cells were treated with different concentrations of FCZ and DPIC for three overnight incubations, then cells were spotted on agar and allowed to incubate 24 hours before growth recovery was assessed. A DMSO control experiment was performed in parallel.

Saccharomyces cerevisiae

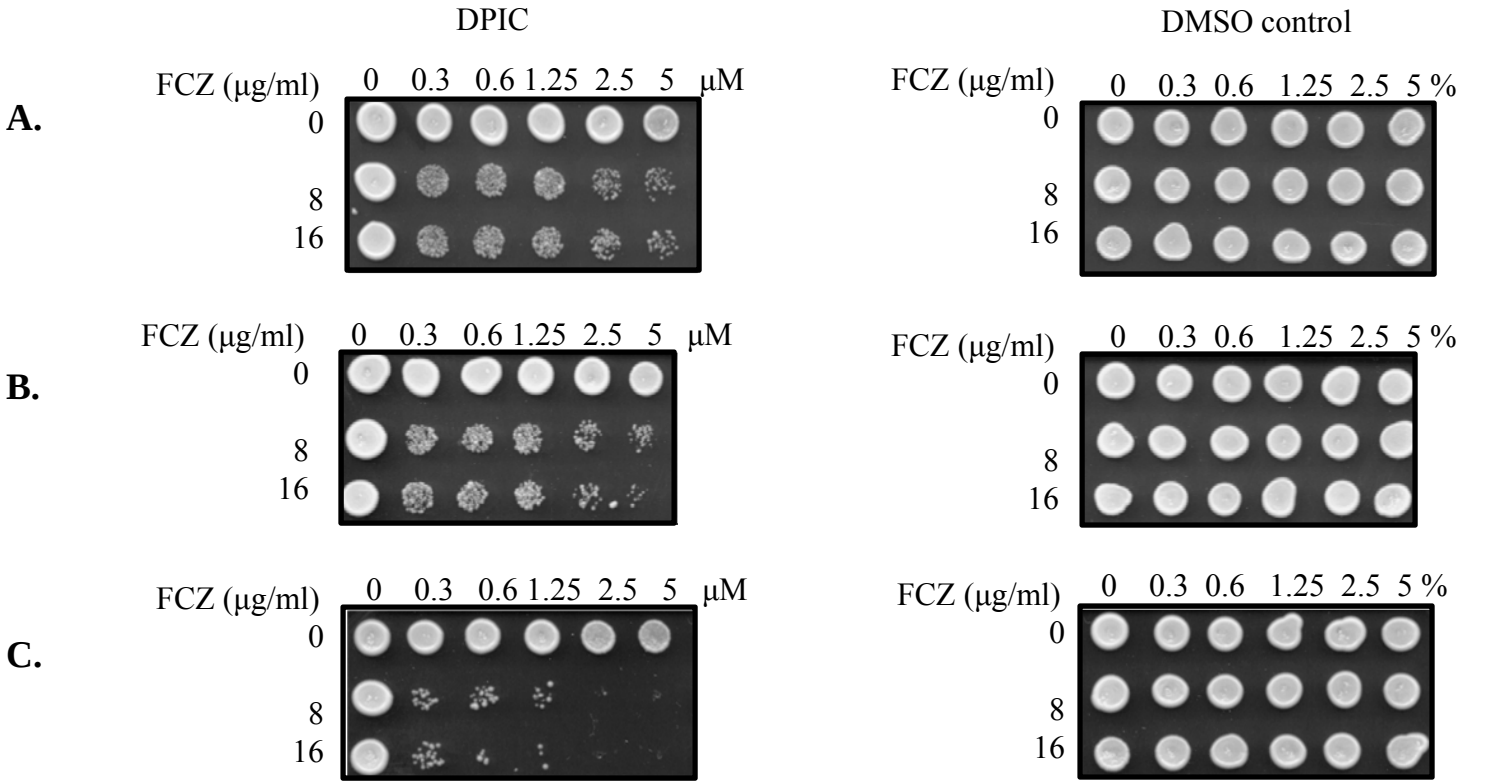

Candida albicans

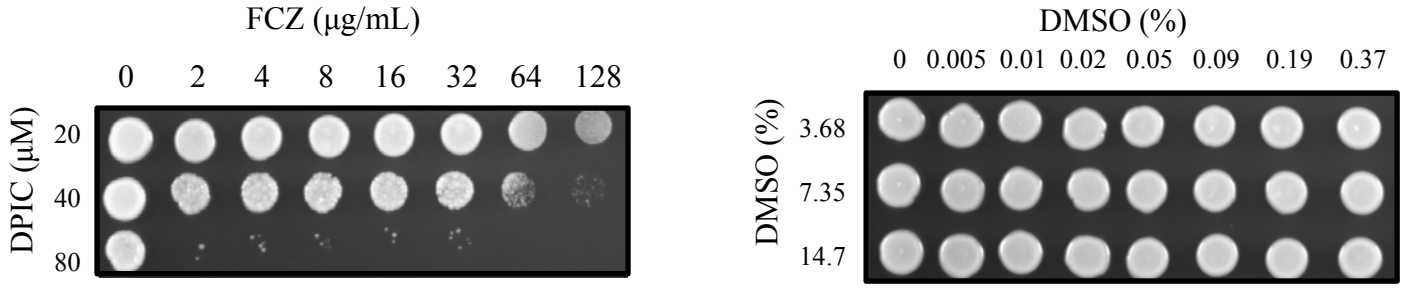

Table 8a SGA deletion strains exhibiting sensitivity to DPIC.

Gene descriptions from www.yeastgenome.org.

Systematic name	Gene name	Gene description
YDR359C	*VID21/ EAF1**	Component of the NuA4 histone acetyltransferase complex
YDR334W	*SWR1**	Swi2/Snf2-related ATPase that is the structural component of the SWR1 complex, which exchanges histone variant H2AZ (Htz1p) for chromatin-bound histone H2A
YDR485C	*VPS72**	Htz1p-binding component of the SWR1 complex, which exchanges histone variant H2AZ (Htz1p) for chromatin-bound histone H2A; required for vacuolar protein sorting
YNL106C	*INP52*	Phosphatidylinositol 4,5-bisphosphate 5-phosphatase, synaptojanin-like protein with an N-terminal Sac1 domain, plays a role in endocytosis; hyperosmotic stress causes translocation to actin patches
YPL145C	*KES1*	Member of the oxysterol binding protein family, which includes seven yeast homologs; involved in negative regulation of Sec14p-dependent Golgi complex secretory functions, peripheral membrane protein that localizes to the Golgi complex
YDR378C	*LSM6**	Lsm (Like Sm) protein; part of heteroheptameric complexes (Lsm2p-7p and either Lsm1p or 8p): cytoplasmic Lsm1p complex involved in mRNA decay; nuclear Lsm8p complex part of U6 snRNP and possibly involved in processing tRNA, snoRNA, and rRNA
YGL244W	*RTF1**	Subunit of the RNA polymerase II-associated Paf1 complex; directly or indirectly regulates DNA-binding properties of Spt15p and relative activities of different TATA elements; involved in telomere maintenance
YPL226W	*NEW1**	ATP binding cassette family member; Asn/Gln-rich rich region supports [NU+] prion formation, susceptibility to [PSI+] prion induction and aggregation of a fragment of the human Machado-Joseph Disease protein

* Interact together, either directly or through another gene present in the list.

Table 8b FCZ-fungicidal genes which interact with DPIC sensitive strains.

DPIC sensitive strain	FCZ-fungicidal strain
VID21	*TFP1, GCN5*
SWR1	*NUP84, NGG1, VPH2*
VPS72	*NUP84, NGG1, SSN3*
LSM6	*VPH2, MED2, SSN3, NGG1, SRB8, NUP84, BEM2*
NEW1	*SRB8*

DPIC, wild type cells were inoculated into three different media, synthetic complete 3% glycerol, synthetic complete pH 8, and synthetic complete supplemented with 50mM $CaCl_2$, and were treated with DPIC concentrations of 125, 250 and 500μM as well as with a DMSO control. The vma^- phenotype is characterized by an inability to grow on non-fermentable carbon sources, elevated pH and elevated calcium concentrations (Sambade, 2005, Oluwatosin, 1998, Graham, 2003), consequently if DPIC is targeting *VMA* genes, growth in these media should be limited or non-existent. For cells inoculated in 3% glycerol SC media and SC media with pH 8, cell growth was present only for the DMSO controls; if DPIC was present no cell growth was observed (Figure 14). Cells incubated in media supplemented with $CaCl_2$ grew to lower levels when DPIC was added to the media.

Figure 14. Wild type cells treated with DPIC result in vma$^-$ phenotype

A. Since the *FIT2* gene used to construct the reporter gene which identified DPIC as a fungicidal synergistic counterpart to fluconazole was significantly up-regulated in the *vma* deletion strains, DPIC's target is suggested to be a component affecting the V-ATPase complex. Showing that DPIC causes a vma$^-$ phenotype when treating wild type cells, supporting the notion that it affects the V-ATPase function, completes the circle of the strategic approach taken.

B. Liquid cultures of wild type cells were treated with DPIC (125, 250 and 500μM), or the DMSO control, in 3% glycerol synthetic complete media and synthetic complete media at pH8.

C. YPD agar plate spotted with 2μL of each culture depicted in **B**.; used to monitor cell recovery once the drug is removed. The cells were spotted after three overnight incubations.

A.

23 ΔFCZ deletion strains

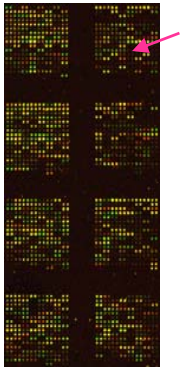

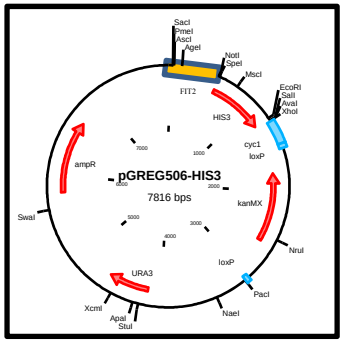

ΔFCZ strain | Wild type strain

H D | H D

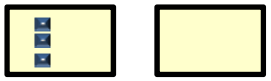

Growth | No growth | No growth

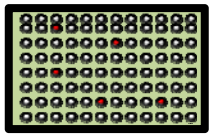

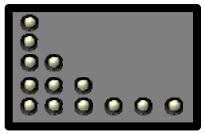

Synthetic complete 3% glycerol

Synthetic complete 2% dextrose pH8

B.

DMSO

DPIC

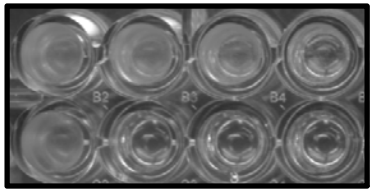

DMSO

DPIC

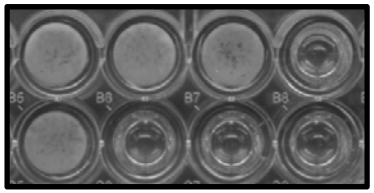

C.

DMSO

DPIC

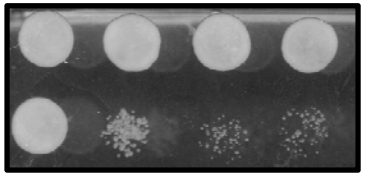

DMSO

DPIC

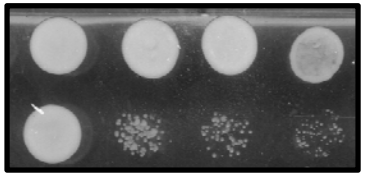

Chapter 4

Discussion

A complete understanding of how cells are affected by fluconazole (FCZ), the most commonly used antifungal, would provide insight on possible targets for drugs to be used in combination with it. We screened for genes that are essential in the presence of FCZ. We screened the entire non-essential haploid deletion collection with a concentration of FCZ which inhibits growth of the wild type but does not kill the cells (that is, it is fungistatic). In addition to the hypomorphic strain *erg11*, twenty-two of these non-essential genes were determined to be essential for cell survival when exposed to FCZ; these 23 strains were termed FCZ-fungicidal. Their functions are likely to be involved in the cell's response to the drug and perhaps in its processing. From published data, other transcriptional profiles generated demonstrate that the majority of the FCZ-fungicidal genes are required in response to a variety of other stresses and that they seem to play a role in the adaptation to chemical stresses (Gasch, 2000). Most of the 23 genes are also required in the presence of compounds whose targets do not involve the ergosterol biosynthesis pathway. The hypomorphic *erg11* strain is killed by low concentrations of FCZ which demonstrates the importance of the amount of drug versus its target. The reason why these genes become essential in the presence of FCZ could be due to the cell's inability to deal with the accumulation of toxic compounds or intermediates which causes growth arrest and cell death. The set of FCZ-fungicidal genes can be divided into different functional complexes: the SAGA complex, the mediator complex, the cell wall/cytoskeleton complex, and the V-ATPase complex.

When exposed to FCZ, the cells from the subset of the 23 FCZ-fungicidal deletion strains that are involved in transcriptional regulation (SAGA and Mediator complexes) might not be able to produce the necessary proteins, whether in sufficient quantities or at a rapid enough rate, to respond to the presence of the drug. The pleitropic drug pump *PDR5*, whose transcription requires recruitment of the SAGA and mediator complexes to its promoter (Gao, 2004), is responsible for pumping FCZ out of the cell. An assay involving the stain

Rhodamine 123 demonstrated that in the absence of the genes belonging to the SAGA and mediator complexes, the dye specifically exported by Pdr5p accumulated in the cells after washout. These results support the hypothesis that impaired activity of the SAGA or mediator complex may lead to reduced levels of Pdr5p which are insufficient to pump FCZ out of the cell.

The FCZ-fungicidal deletion strains involved in the V-ATPase complex are suggested to ineffectively deposit FCZ into the vacuoles. This hypothesis was proposed after staining the 23 FCZ-fungicidal strains with the dye FUN1. The V-ATPase deletion strains demonstrated ineffective deposit of the dye in the vacuole which suggests a similar response when cells treated with FCZ. The *vma* mutants might not alleviate the cell of FCZ as well as the wildtype strain and consequently cells might not survive due to the overwhelming presence of the drug.

Genes *GCS1*, *SLT2*, *SAC6,* and *BEM2* are involved in maintaining and organizing the cell wall or cytoskeleton. The absence of these genes may cause cells to exhibit compromised skeletal/cell walls which, in turn, could render them susceptible to a drug targeting the fungal plasma membrane. The importance of maintaining cell wall/cytoskeletal and membrane integrity simultaneously is emphasized by genetic interactions indicating that in the absence of cell structure genes, negative effects on *ERG11* are observed. As demonstrated by the *erg11* hypomorphic strain, compromised levels of *ERG11* allow FCZ to go from a fungistatic antifungal agent to a fungicidal one. This would explain how the cytoskeletal/cell wall class of deletion strains become essential in the presence of FCZ.

Microarray analysis was performed on all 23 FCZ-fungicidal strains and compared with the wild type strain. The dendogram in Figure 4 shows the correlation between the transcriptional profiles generated. The expression profiles for the dye swapped deletion strains performed on different days (dye-swaps) clustered together as well as deletion strains

belonging to the same complex. As expected, genes with similar functions provided similar expression profiles. There are some exceptions where the dye swaps for the same deletion strain did not cluster together. For example deletion strains Δ*slt2*, Δ*gcs1* and Δ*thr1* whose microarray analysis was performed on March 30th 2007, clustered together instead of to their respective dye swap expression profile. The reason for this is because there were some slight day effects which bias the expression profiles. This caused microarray analyses done on the same day to appear more similar to each other than to the corresponding gene's expression profile from a different day. This is a general problem with microarray analysis and while there are preventive measures such as working in ozone-free tents, dipping the microarrays in anti-oxidant solutions or even not performing microarray analysis on days where ozone levels may be elevated, it is difficult to completely avoid slight day effects (Fare, 2003).

Microarray analysis was also performed on the Δ*pdr5* deletion strain exposed to FCZ compared to the untreated wild type strain. Expression profiles were generated for 90- and 180-minute treatments with FCZ. As demonstrated in Table 4, the ergosterol pathway, known to be targeted by azole compounds, represented the greatest number of up-regulated genes after exposure to FCZ. A group performed a series of studies investigating gene expression changes when cells were exposed to five different azoles, including FCZ (Bammert, 2000). Bammert *et al.* reported five genes to be significantly up-regulated after exposure to the antifungals which correlate with the results obtained in this study: *ERG2*, *ERG3*, *ERG6*, *ERG9*, and *ERG11*. Although there was no reference made to genes *ERG26*, *ERG27*, and *ERG28*, which were over-expressed in the current study, the focus of Bammert *et al*.'s work did not involve these genes and only genes up-regulated in all five drug profiles were highlighted. Bammert *et al*. reported *ERG1* not to be significantly over-expressed upon azole treatment, although in this study it is. However, they also concluded that exposure to terbinafine, which directly targets Erg1p, did not trigger *ERG1* up-regulation. Since the study

was published in 2000 when microarray technology was in its infancy, it is possible that the up-regulation of *ERG1* was masked due to the quality of the arrays.

Bioinformatics analysis of the microarray data provided insight on what processes were significantly differentially expressed among all the deletion strains and which were specific to certain classes. To determine common processes which occur across the 23 FCZ-fungicidal deletions which could account for the cell's susceptibility to FCZ, their expression profiles were compared to those of the FCZ treated Δ*pdr5* deletion strain (Figure 5). The heatmap generated consists of gene-ontology (GO) categories (www.geneontology.org) which are differentially expressed in more than two of the expression profiles studied. According to this analysis, the classes which are most strongly affected are ion transport, amino acid metabolism/biosynthesis, ATP synthesis coupled electron transport and ergosterol/sterol biosynthesis/metabolism. Although this signature heatmap provides information on the biological categories most significantly affected by FCZ treatment and in the FCZ-fungicidal deletion strains, more knowledge on which categories are over- or under-expressed would be required to provide insight into how the cells are responding.

More specific investigation into over-represented up-regulated classes provided a more detailed analysis which is shown in Figures 6. The first noticeable result is the wide red band representing the following processes: amino acid metabolism, amino acid and derivative metabolism, amine metabolism, nitrogen compound metabolism, amine biosynthesis, nitrogen compound biosynthesis, and amino acid biosynthesis. These categories are up-regulated for almost every FCZ-fungicidal strain and in both FCZ treatment profiles. An explanation for the over-expression of these classes is that the cells are under stresses related to nitrogen limitations. Nitrogen sources are essential for cell viability; they include amino acids required for the production of proteins and in fungal cells, nitrogen sources are needed for the synthesis of cell wall components. Good nitrogen sources (which are characterized as

being easily converted into glutamate and glutamine) such as glutamine, asparagines, and ammonium (Boer, 2007), are selectively used by yeast cells in preference to poor ones such as proline. When the cell has used up all the good nitrogen sources, it will undergo nitrogen limitation and then take up poor nitrogen sources.

In a recent article, microarray analysis was performed on cells grown on L-leucine, which is not a very good nitrogen source, and compared to cells grown on good nitrogen source ammonia. The significantly represented GO-annotated groups that were identified when comparing the two profiles included amino acid biosynthesis, amine biosynthesis, and aromatic amino acid metabolism (Schoondermark-Stolk, 2006) which are very similar to those observed in this study.

An intact cytoskeleton has been reported to be required for nuclear accumulation of nitrogen catabolic repression (NCR)-sensitive transcription factor Gln3 in response to nitrogen limitation (Cox, 2004). The movement of Gln3 from the cytoplasm to the nucleus occurs when cells go from good to poor nitrogen sources. When the actin skeleton is compromised, as is possible for some FCZ-fungicidal strains, Gln3 remains in the cytoplasm. Although the cells are nitrogen deprived, the transcription activator does not trigger the appropriate cell response.

Additionally, cells lacking the Vma4p show aberrant actin organization, suggesting a possible link between the V-ATPase and formation or maintenance of the cytoskeleton (Kane, 2006). It has been also reported that the stability of the Vma4p protein depends on the presence of the *VMA10* gene product, another FCZ-fungicidal member (Zhang, 1998). This information suggests that the up-regulation of amino acid biosynthesis and metabolism categories can in part be accounted for by a weakened cytoskeleton caused by either the deletion of genes directly involved in its maintenance or the V-ATPase complex which indirectly affects it. Another argument that might explain this up-regulation is that chitin and

glycoproteins depend on nitrogen sources for their synthesis. Thus, if the cell wall is compromised in the FCZ-fungicidal strains and FCZ treated cells, an increase in demand for nitrogen sources to reinforce it, would be expected.

Ergosterol has been proven to be required for targeting the tryptophan permease, Tat2p, to the yeast plasma membrane (Umebayashi, 2003). In wild type cells, Tat2p is transported to the vacuole to be degraded under high tryptophan conditions. In the Δ*erg6* mutant, Tat2p is missorted to the vacuole under low tryptophan concentrations. This outcome may occur in cells exposed to FCZ and FCZ-fungicidal strains with compromised ergosterol pathways, causing improper transport of amino acids.

In yeast cells, one of the functions of the vacuole is storage of metabolic building blocks such as nitrogen sources. Therefore, it is not surprising that an up-regulation in nitrogen sources is observed in *vma* mutants. However, there are other possible explanations for the over-expression detected here. There are two classes of amino acid permeases: general amino acid permeases (e.g. GAP1) and constitutive permeases (e.g. TAT2). Both classes of permeases are transported to the vacuole for degradation under different circumstances. Gap1p is sorted to the vacuole when ample amounts of good nitrogen sources are present, whereas, Tat2p is transported to the vacuole upon nitrogen deprivation. This implies that at all times, permeases are targeted to the vacuole for degradation. *vma* mutants have been reported to exhibit overall lower levels of vacuolar protease activity and their maturation rate is lower than in wild type strains (Kane, 2006). This deficiency in protease activity is enough to slow down the vacuolar proteolysis induced by starvation. It has been shown that, in a mutant strain lacking vacuolar proteases, Tat2p was completely resistant to induced degradation (Beck, 1999). Improper degradation of permeases in *vma* mutants would cause their over-accumulation in the cell, resulting in the disruption of amino acid transport.

Also, it has been suggested that when cells are faced with limited nitrogen sources, one option is to change the transmembrane potential to change the Km of nitrogen transporters (Usaite, 2006). In doing so, the cells could lower the cytosolic proton concentration through acidification of the vacuole. The V-ATPase complex in the Δ*vma* mutants inefficiently acidifies its vacuoles and this could affect the cell's ability in amino acid uptake when faced with nitrogen deprivation. It should be noted that *BAP2*, a branched-chain amino acid permease necessary for the transport of amino acids, was up-regulated in all *vma* deletion strains. No permease was significantly up-regulated in any other FCZ-fungicidal strain.

At the top of Figure 6, the FCZ treatment profile, as expected, has a very strong over-expression of the following processes: sterol biosynthesis, steroid biosynthesis, steroid metabolism, sterol metabolism, ergosterol metabolism, and ergosterol biosynthesis. The only other deletion strains which parallel this up-regulation are the deletion strains from the V-ATPase class. Since FCZ targets the ergosterol pathway, an up-regulation in categories involved in that pathway is expected. The high level over-expression observed for the Δ*vma* genes implies that a compromised V-ATPase complex can directly affect the ergosterol pathway. As demonstrated by the *erg11* hypomorphic strain, an impaired the ergosterol pathway leads to an increase in the potency of FCZ. Ergosterol delivery to wild type vacuoles stimulates their *in vitro* fusion. Vacuoles in strains with compromised ergosterol pathways require the addition of sterol: in the absence of the ergosterol pathway there is marked vacuole fragmentation (Kato, 2001). It has been recently proposed that Dap1, a heme-binding protein that activates Erg11, regulates vacuolar structure via sterol biosynthesis (Craven, 2007). Vacuolar defects have been observed for deletion strain Δ*dap1* displaying the close tie between Dap1 and the vacuole structure. Given this information, the following hypothesis is proposed: the ergosterol/sterol biosynthesis pathway is up-regulated to stabilize the

compromised vacuoles in the Δ*vma* deletion strains.

There is a significant up-regulation for the categories involved in ion homeostasis among the Δ*vma* deletion strains (bottom right corner of Figure 6). This is a relevant observation which ties in with a discovery that was made across all Δ*vma* deletion strains. The microarray analysis of the 23 ΔFCZ-fungicidal strains revealed that the most significantly up-regulated genes were involved in iron transport and homeostasis and the greatest over-expression occurred in the V-ATPase deletion strains (Figure 7). As can be noticed in Figure 7, numerous genes involved in the GO-annotated biological processes iron metabolism, cellular iron ion homeostasis, iron ion transport, and siderophore transport demonstrate significant up-regulation almost solely restricted to the Δ*vma* deletion strains. *FIT2* is the most over-expressed gene and is not only robustly up-regulated in the Δ*vma* deletion strains but also for Δ*srb8*, Δ*ssn3* and FCZ treatment for 180 minutes. These results are not surprising given that the literature has demonstrated over-expression of genes involved in iron transport and homeostasis among *vma* mutants (Milgrom, 2007). However, this iron related gene up-regulation has not been reported as extensively as here. A hypothesis for these observations is that the cells exhibit defective copper loading of apoFet3p, which occurs in a post-Golgi compartment and requires an acidic pH (Davis-Kaplan, 2004). The V-ATPase complex is responsible for the acidification of organelles and in *vma* mutant strains the pH might not be low enough to meet apoFet3p's requirements. Fet3p is a multicopper oxidase which is responsible for high-affinity iron uptake (Stoj, 2006). Without a functional Fet3p, there will be a lack of iron uptake.

Although it has been suggested that iron is required in the detoxification of lanosterol and iron depletion has been shown to be toxic to cells containing elevated levels of lanosterol (Craven, 2007), there were very few up-regulated iron-related genes observed in the FCZ treatment profiles. However, since the cells were exposed to FCZ a maximum of 180 minutes

in this study, it could be too short a timeframe for lanosterol to accumulate to levels which would deplete the cell's iron stores.

Unlike the up-regulation heatmap where at least the Δ*vma* genes paralleled the FCZ treatment profile, there is no real correlation for the down-regulated genes (Figure 8). However, there is common down-regulation among the same FCZ-fungicidal gene classes on the heatmap. For example, Δ*srb8* and Δ*ssn3* parallel each other's profile, as well as Δ*slt2*, Δ*bem2,* and Δ*gcs1*. As always, the Δ*vma*s have parallel expression profiles.

The Δ*vma* deletion strains caused a significant down-regulation in the following GO categories: organelle ATP synthesis coupled to transport, electron transport, and oxidative phosphorylation. The electron transport chain that pumps protons across the mitochondrial membrane to generate ATP through oxidative phosphorylation, uses iron-sulfur (FeS) clusters as electron carriers. The V-ATPase complex was identified as a major player in the uptake and distribution of multiple types of different metals (Eide, 2005). If the V-ATPase complex, which is compromised in the *vma* mutants, is responsible for distributing the iron required for the FeS cluster, it could account for the dramatic down-regulation in ATP synthesis coupled to electron transport associated with these deletion strains.

From the microarray analysis, highly up-regulated genes with low expression levels in the wild type strain were sought out to generate a growth reporter that would signal the inactivation of a FCZ-fungicidal gene or protein. Figure 9 displays a heatmap of the most significantly up-regulated genes across all FCZ-fungicidal expression profiles. From this analysis the most highly up-regulated genes were determined to *FIT2* and *FIT3* whose gene products are both mannoproteins incorporated in the cell wall. The gene *YLR162W* was also strongly over-expressed according to Figure 9.

Using bioinformatics tools to predict which significantly up-regulated genes would generate good reporter genes for our assay, two different assessments were made based on

the expression of these genes in other yeast expression profiles (Tables 5 and 6). Because the ideal reporter would be specifically up-regulated in response to the gene deletion, we expect the reporter gene to be up-regulated when any of its target genes (i.e. the genes that are to be reported on) are down-regulated. Thus, the true positive rate is the fraction of profiles in which the reporter gene is up-regulated when its target genes are down-regulated. The false positive rate is the fraction of profiles in which the reporter gene is up-regulated when its target genes are not down-regulated. The false negative rate is the fraction of profiles in which the target genes are down-regulated yet the reporter gene is not up-regulated.

Table 5 summarizes the assessment of candidate reporters based on the up- or down-regulation fold change alone. Table 6 summarizes the assessment of candidate reporters based on fold change together with the differential expression p-values. The candidate genes which are predicted to be best are the ones with the lowest false positive rate. A low false positive rate is ideal for avoiding the validation of false hits from a drug screen. Although it could be considered risky not to take p-values into consideration, many of the expression profiles in this analysis were generated in the year 2000 at the beginning of microarray technology when signals tended to be noisy and analyses rudimentary. Because of this, down-regulation was more difficult to detect than up-regulation and, consequently, interesting down-regulated genes could be masked by not being considered significant when including p-values in the analysis. Moreover, only 58% of the collected profiles had associated p-values. Focusing on this subset reduces the number of profiles with which a candidate reporter can be assessed and the resulting error estimate is therefore less likely to be accurate. This is apparent through the extreme error rates in Table 5. i.e. 0 may simply indicate 0/1, NA indicates no profiles were available for a particular error computation. This is why two assessments of the candidate reporters have been made.

Applying the information obtained from Figure 9 and the bioinformatics prediction,

three reporters were chosen to be investigated in depth: *FIT2*, *CIT2*, and *YLR162W*. The fold change of these three genes across the FCZ-fungicidal strains is presented in Table 6. Although the three genes were predicted to provide the best reporters, only the *FIT2* reporter behaved as expected. The *FIT2* reporter was activated in deletion strains where the *FIT2* gene was determined to be up-regulated by the microarray analysis (Δ*vma*s) and not in strains where *FIT2* was shown to be down-regulated. Additionally, the reporter was not activated in heterozygous diploid Δ*vma* deletion strains.

Reporters *CIT2* and *YLR162W* either showed growth for the haploid and diploid strains or did not grow for the haploid strains in the absence of histidine and presence of 3-AT. The *CIT2* reporter was determined to be significantly leaky because whether it was transformed into the haploid deletion strains where it should be activated (Δ*vma*s and Δ*spt20*) or the heterozygous diploid deletion strain where it should not be activated, it always remained activated. In contrast, the *YLR162W* reporter was not activated in any of the deletion strains in which it had been shown to be up-regulated (Δ*gcs1*, Δ*thr1*, and Δ*vph2*). This observation can be justified by the *YLR162W* promoter being too stringent. The method used to generate the reporter is valid as the plasmid DNA for both of these reporters was extracted, digested, and confirmed by sequence analysis to be the expected construct. These results demonstrate that the ideal reporter will be gene specific and the method that best predicts which gene promoter to use is one where p-values are not taken into consideration.

Upon investigating into compounds which specifically induce the *FIT2* reporter, the Sigma LOPAC library was screened. One compound was determined to reproducibly and robustly activate the reporter: DPIC. In assessing the reporter's ability to identify fluconazole synergistic fungicidal compounds, the Sigma LOPAC library was also screened with a sub-lethal concentration of FCZ (10μg/mL) using wild type cells. Approximately thirty compounds to prevented or slowed cell growth in the presence of FCZ. Upon further

investigation, four compounds, DL-erythro-dihydrosphingosine, MG 624, DPIC, and calmidazolium chloride, which had prevented cell growth for several days in liquid, were tested by the checkerboard method. The only compound determined to be a synergistically fungicidal with FCZ was DPIC. The other compounds demonstrated additive effects or fungistatic synergy. Thus, the *FIT2* reporter specifically selected the only compound from the library which acts synergistically with FCZ causing cell death.

A drawback to the *FIT2* reporter is its sensitivity to DMSO, a solvent commonly used to dissolve compounds. At concentrations above 0.05% DMSO, the *FIT2* reporter is up-regulated. Consequently, the highest compound concentration which can be used for our assay is 1μM because the stock concentration is 2mM and the final assay volume used is 200μL. It could be argued that compounds of interest could go unnoticed due to the low concentration of compounds used in the screening process. Future work on this project involves generating a modified reporter which will have multiple binding sites for *FIT2*'s transcription factor *AFT1*. This concept of a reporter with additional transcription factor binding sites has been shown to provide better stimulated-to-basal signal ratios (Tatebayashi, 2006). With additional *AFT1* binding sites, the *FIT2* reporter could be more robust and display a decreased sensitivity to the different stresses it is subjected to, such as DMSO.

The most interesting finding with this reporter is that its ability to specifically identify FCZ synergistic fungicidal compounds in *Saccharomyces cerevisiae* is also paralleled in the virulent species *Candida albicans* (Figure 13). Although the concentration of DPIC required for fungicidal synergy with FCZ is greater in *Candida albicans* than in *Saccharomyces cerevisiae*, it only necessitates 8μg/mL of FCZ and 80μM of DPIC to kill C. *albicans* cells whereas 128μg/mL of FCZ alone does not kill them. It is remarkable that such small quantities of drug have fungicidal activity with FCZ. It is important to note that DPIC alone does not affect cell growth, it requires the fungistatic activity of FCZ to affect the cells.

The advantage to this reporter assay is that not only are fluconazole synergistic fungicidal compounds identified but the drug's target is also simultaneously identified. Because the *FIT2* reporter was activated by DPIC, the theory behind the reporter assay would suggest that DPIC's target in *S. cerevisiae* would be part of the V-ATPase complex or genes that affect it. In attempting to determine DPIC's target in *Saccharomyces cerevisiae*, the SGA deletion collection was screened on agar plates containing sub-lethal concentrations of the drug. Upon retesting, eight sensitive genes were obtained (Table 7a). All eight of these genes have *Candida albicans* homologs. Interestingly, six of the eight genes interact together; *VID21*, *SWR1,* and *VPS72* all interact together, *VPS72* and *SWR1* interact with *RTF1*, *VPS72* interacts with *LSM6* which interacts with *NEW1*. They interact together with or as part of the SWR1 complex, which catalyzes the exchange of H2A.Z to replace histone H2A within intact nucleosomes. (Wu, 2005)

The six genes which interact together also interact with vacuolar genes, either Vacuolar Protein Sorting (vps) or VACuole related (vac) genes. Additionally, except for *RTF1*, they each have been shown to interact with at least one FCZ-fungicidal gene (Table 7b). Although the literature describes these genes as interacting together, there is not much information on how and why these interactions occur. Recently, H2A.Z has been shown to act as a molecular identifier of recently repressed genes and promote their retention at the nuclear periphery (Brickner, 2007). The SWR1 complex interacts very closely to H2A.Z, which could explain for the interactions reported between the genes involved in the SWR1 complex and *NUP84*. *GCN5* and *NGG1* are subunits of histone acetyltransferase complexes and provide a way in which they could interact with SWR1. *MED2*, *SSN3* and *SRB8* are subunits of the mediator complex which plays a central role in the assembly of the preinitiation complex (Carey, 2005). Since this process occurs alongside chromatin remodelling there could be the opportunity for genes associated with the SWR1 complex to

interact with *MED2*, *SSN3,* and *SRB8*. In fact, using ChIP-chip analysis to map H2A.Z across the yeast genome with a 300-bp resolution, Guillemette *et al.* discovered the Z locus is within the promoter of the *SRB8* gene. (Guillemette, 2005) The gene *BEM2* was also found to interact with the SWR1 complex. This interaction likely occurs with the gene *ACT1* which is part of the SWR1 complex (Krogan, 2004) and reported to interact with *BEM2* (Wang, 1995). In Biogrid (Stark, 2006), components from the SWR1 complex are shown to interact with *TFP1* and *VPH2*; in fact they belong to an entire network of interacting genes. In the literature, however, no such biological interactions have been reported. The explanation for this is that these interactions were established by an E-MAP published in 2007 (Collins, 2007) and supporting biological data does not exist yet.

From these results, however, the conclusion can be made that DPIC targets genes associated with the SWR1 complex and this complex interacts with a number of FCZ-fungicidal genes. Thus, DPIC could be disturbing the target FCZ-fungicidal genes through the SWR1 complex which would explain its synergy with FCZ.

Another assay was performed in attempting to confirm DPIC's involvement with the V-ATPase complex. Wild type cells were incubated with different concentrations of DPIC in media which specifically affect the vma$^-$ phenotype: 3% glycerol SC media, SC media at pH8, and SC media supplemented with 50mM $CaCl_2$. *vma* mutants have been reported to have slow or inhibited growth in the media mentioned above (Sambade, 2005, Oluwatosin, 1998, Graham, 2003), thus if DPIC targets the V-ATPase complex in the wild type cells, no or little growth should be observed compared to the DMSO control. The results obtained showed that cells incubated in 3% glycerol SC media and SC media pH8 did not grow if DPIC was present while DMSO controls had abundant cell growth (Figure 14). The results for cells incubated in media supplemented with $CaCl_2$ cannot be confirmed. Although cell growth was less in the presence of DPIC, further studies must be performed before providing

a conclusive result. A hypothesis for the cells' decreased sensitivity to calcium supplementation compared to the non-fermentable carbon source and elevated pH is that DPIC's effect on the V-ATPase complex does not extensively affect calcium export from the cell. Loss of V-ATPase activity leads to the loss of function of Vcx1p encoding the Ca^{2+}/H^{+} antiporter. However, other factors have been suggested to play a role in the calcium sensitivity exhibited by *vma* mutants (Kane, 2006) and DPIC may not be affecting these processes. The fact that the vma^{-} phenotype was produced upon the addition of DPIC suggests that it targets functions affecting the V-ATPase complex. Hence, these results confirm that the reporter assay allows for simultaneous identification of fungicidal synergistic compounds and their drug targets.

Although DPIC has been the key player in proving that the hypothesis and theory behind the novel reporter assay is correct, it cannot be used to treat patients with fungal infections. DPIC is described as a potent and reversible inhibitor of nitric oxide (NO) synthetase in macrophages and endothelial cells. The compound is known to inhibit other flavoenzymes such as neutrophil NADPH oxidase (www.sigmaaldrich.com). Thus DPIC would be toxic if administered to humans. However, since the reporter assay is now known to specifically identify FCZ synergistic fungicidal compounds, the next step is to screen more compound libraries to find a compound which will not be toxic to humans.

Screening for compounds that will act synergistically with FCZ rendering the combination fungicidal is a novel strategy for the development of new combinatorial antifungals. Many attempts to identify such compounds have involved the screening of large random libraries, yet often without obtaining a single true positive compound. Here we have demonstrated that pursuing combination therapies is a promising avenue for combating fungal morbidity while traditional brute force screening has shown to be disappointingly labour intensive and unfruitful.

The application of the novel reporter assay described here can be applied to many other fields. Essentially, we have developed a reporter assay which identifies compounds that inactivate non-essential genes which become essential in the presence of a compound. This same approach could be used, for example, in cancer research to discover compounds which could inhibit genes which indirectly cause uncontrolled cell proliferation. For example, it has been suggested that identifying a specific inhibitor of the enzyme T-cell protein tyrosine phosphatase (TC-PTP) could lead to a novel therapeutic drug used to treat cancer (Bourdeau, 2004). TC-PTP is involved in the negative regulation of surface receptor signalling. Among the various roles it occupies, it has been shown to exert a positive regulation on cell proliferation through the nuclear factor-kappa B (NFκB) pathway (Bourdeau, 2004). NFκB regulates the expression of inflammatory and oncogenic genes (Farrow, 2002, Hanada, 2002). It has been suggested that by inhibiting TC-PTP, the activation of NFκB could be delayed through the decreased activity of inhibitors of kappa-B (IκB) and reduce the possibility of skin cancer (Dajee, 2003). By using a similar strategic approach to the one described here, a specific inhibitor to TC-PTP could be identified. In achieving this, microarray analysis could be performed on cell lines with ineffective TC-PTP and highly up-regulated genes would be monitored. These over-expressed genes would then be used to generate a reporter which would be activated in the absence of TC-PTP function. Chemical libraries would be screened using the reporter, identifying compounds which specifically inhibit TC-PTP.

Here, a novel reporter assay has been described which is able to specifically identify FCZ synergistic compounds in both *S. cerevisiae* and *C. albicans* and simultaneously identify the compound's drug target. This is a revolutionary assay which can be used for a broad spectrum of applications.

References

1. Adams, A. E., D. Botstein, et al. (1991). "Requirement of yeast fimbrin for actin organization and morphogenesis in vivo." Nature **354**(6352): 404-8.

2. Akins, R. A. (2005). "An update on antifungal targets and mechanisms of resistance in Candida albicans." Med Mycol **43**(4): 285-318.

3. Albertson, G. D., M. Niimi, et al. (1996). "Multiple efflux mechanisms are involved in Candida albicans fluconazole resistance." Antimicrob Agents Chemother **40**(12): 2835-41.

4. Anderson, J. B., C. Sirjusingh, et al. (2003). "Mode of selection and experimental evolution of antifungal drug resistance in Saccharomyces cerevisiae." Genetics **163**(4): 1287-98.

5. Baker, S. P. and P. A. Grant (2007). "The SAGA continues: expanding the cellular role of a transcriptional co-activator complex." Oncogene **26**(37): 5329-40.

6. Bammert, G. F. and J. M. Fostel (2000). "Genome-wide expression patterns in Saccharomyces cerevisiae: comparison of drug treatments and genetic alterations affecting biosynthesis of ergosterol." Antimicrob Agents Chemother **44**(5): 1255-65.

7. Beck, T., A. Schmidt, et al. (1999). "Starvation induces vacuolar targeting and degradation of the tryptophan permease in yeast." J Cell Biol **146**(6): 1227-38.

8. Bennett, J. E., W. E. Dismukes, et al. (1979). "A comparison of amphotericin B alone and combined with flucytosine in the treatment of cryptoccal meningitis." N Engl J Med **301**(3): 126-31.

9. Blader, I. J., M. J. Cope, et al. (1999). "GCS1, an Arf guanosine triphosphatase-activating protein in Saccharomyces cerevisiae, is required for normal actin cytoskeletal organization in vivo and stimulates actin polymerization in vitro." Mol Biol Cell **10**(3): 581-96.

10. Boer, V. M., S. L. Tai, et al. (2007). "Transcriptional responses of Saccharomyces cerevisiae to preferred and nonpreferred nitrogen sources in glucose-limited chemostat cultures." FEMS Yeast Res **7**(4): 604-20.

11. Bourdeau, A, et al. (2004). "Protein Phosphatases." Springer 185-196

12. Brachmann, C. B., A. Davies, et al. (1998). "Designer deletion strains derived from Saccharomyces cerevisiae S288C: a useful set of strains and plasmids for PCR-mediated gene disruption and other applications." Yeast **14**(2): 115-32.

13. Brickner, D. G., I. Cajigas, et al. (2007). "H2A.Z-mediated localization of genes at the nuclear periphery confers epigenetic memory of previous transcriptional state." PLoS Biol **5**(4): e81.

14. Calderone, R. A. and W. A. Fonzi (2001). "Virulence factors of Candida albicans." Trends Microbiol **9**(7): 327-35.

15. Candau, R., J. X. Zhou, et al. (1997). "Histone acetyltransferase activity and interaction with ADA2 are critical for GCN5 function in vivo." Embo J **16**(3): 555-65.

16. Cappelletty, D. and K. Eiselstein-McKitrick (2007). "The echinocandins." Pharmacotherapy **27**(3): 369-88.

17. Carey, M. (2005). "Chromatin marks and machines, the missing nucleosome is a theme: gene regulation up and downstream." Mol Cell **17**(3): 323-30.

18. Choi, E. H., C. B. Foster, et al. (2003). "Association between chronic disseminated candidiasis in adult acute leukemia and common IL4 promoter haplotypes." J Infect Dis **187**(7): 1153-6.

19. Clark, T. A. and R. A. Hajjeh (2002). "Recent trends in the epidemiology of invasive mycoses." Curr Opin Infect Dis **15**(6): 569-74.

20. Cleary, J. D., S. W. Chapman, et al. (2007). "High purity amphotericin B." J Antimicrob Chemother **60**(6): 1331-40.

21. Collins, S. R., K. M. Miller, et al. (2007). "Functional dissection of protein complexes involved in yeast chromosome biology using a genetic interaction map." Nature **446**(7137): 806-10.

22. Cox, K. H., J. J. Tate, et al. (2004). "Actin cytoskeleton is required for nuclear accumulation of Gln3 in response to nitrogen limitation but not rapamycin treatment in Saccharomyces cerevisiae." J Biol Chem **279**(18): 19294-301.

23. Craven, R. J., J. C. Mallory, et al. (2007). "Regulation of Iron Homeostasis Mediated by the Heme-binding Protein Dap1 (Damage Resistance Protein 1) via the P450 Protein Erg11/Cyp51." J Biol Chem **282**(50): 36543-51.

24. Cuenca-Estrella, M. (2004). "Combinations of antifungal agents in therapy--what value are they?" J Antimicrob Chemother **54**: 854-869.

25. Dajee, M., M. Lazarov, et al. (2003). "NF-kappaB blockade and oncogenic Ras trigger invasive human epidermal neoplasia." Nature **421**(6923): 639-43.

26. Davis-Kaplan, S. R., D. M. Ward, et al. (2004). "Genome-wide analysis of iron-dependent growth reveals a novel yeast gene required for vacuolar acidification." J Biol Chem **279**(6): 4322-9.

27. De Bernardis, F., P. A. Sullivan, et al. (2001). "Aspartyl proteinases of Candida albicans and their role in pathogenicity." Med Mycol **39**(4): 303-13.

28. Denning, D. W. (2002). "Echinocandins: a new class of antifungal." J Antimicrob Chemother **49**(6): 889-91.

29. de Nobel, H., C. Ruiz, et al. (2000). "Cell wall perturbation in yeast results in dual phosphorylation of the Slt2/Mpk1 MAP kinase and in an Slt2-mediated increase in FKS2-lacZ expression, glucanase resistance and thermotolerance." Microbiology **146 (Pt 9)**: 2121-32.

30. Desmoucelles, C., Pinson, B., Saint-Marc, C. and Daignan-Fornier, B. (2002). "Screening the yeast "disruptome" for mutants affecting resistance to the immunosuppressive drug, mycophenolic acid." J Biol Chem **277**: 27036--27044.

31. Dorer, R. K., Zhong, S., Tallarico, J.A., Wong, W.H., Mitchison, T.J. and Murray, A.W. (2005). "A small-molecule inhibitor of Mps1 blocks the spindle-checkpoint response to a lack of tension on mitotic chromosomes." Curr Biol **15**: 1070--1076.

32. Doyon, Y. and J. Cote (2004). "The highly conserved and multifunctional NuA4 HAT complex." Curr Opin Genet Dev **14**(2): 147-54.

33. Eberharter, A., D. E. Sterner, et al. (1999). "The ADA complex is a distinct histone acetyltransferase complex in Saccharomyces cerevisiae." Mol Cell Biol **19**(10): 6621-31.

34. Eggimann, P., J. Garbino, et al. (2003). "Management of Candida species infections in critically ill patients." Lancet Infect Dis **3**(12): 772-85.

35. Egner, R., F. E. Rosenthal, et al. (1998). "Genetic separation of FK506 susceptibility and drug transport in the yeast Pdr5 ATP-binding cassette multidrug resistance transporter." Mol Biol Cell **9**(2): 523-43.

36. Eide, D. J., J. T. Bridgham, et al. (1993). "The vacuolar H(+)-ATPase of Saccharomyces cerevisiae is required for efficient copper detoxification, mitochondrial function, and iron metabolism." Mol Gen Genet **241**(3-4): 447-56.

37. Enloe, B., A. Diamond, et al. (2000). "A single-transformation gene function test in diploid Candida albicans." J Bacteriol **182**(20): 5730-6.

38. Fare, T. L., E. M. Coffey, et al. (2003). "Effects of atmospheric ozone on microarray data quality." Anal Chem **75**(17): 4672-5.

39. Farrow, B. and B. M. Evers (2002). "Inflammation and the development of pancreatic cancer." Surg Oncol **10**(4): 153-69.

40. Fitzgerald, J. B., Schoeberl, B., Nielsen, U.B. and Sorger, P.K. (2006). "Systems biology and combination therapy in the quest for clinical efficacy." Nature chemical biology **2**: 458-466.

41. Gallagher, J. C., C. MacDougall, et al. (2004). "Recent advances in antifungal pharmacotherapy for invasive fungal infections." Expert Rev Anti Infect Ther **2**(2): 253-68.

42. Gao, C., Wang, L., Milgrom, E. and Shen, W.C.W. (2004). "On the mechanism of constitutive Pdr1 activator-mediated PDR5 transcription in Saccharomyces cerevisiae: evidence for enhanced recruitment of coactivators and altered nucleosome structures." J Biol Chem **279**: 42677-42686.

43. Gasch, A. P., P. T. Spellman, et al. (2000). "Genomic expression programs in the response of yeast cells to environmental changes." Mol Biol Cell **11**(12): 4241-57.

44. Gelperin, D. M., M. A. White, et al. (2005). "Biochemical and genetic analysis of the yeast proteome with a movable ORF collection." Genes Dev **19**(23): 2816-26.

45. Ghannoum, M. A. and L. B. Rice (1999). "Antifungal agents: mode of action, mechanisms of resistance, and correlation of these mechanisms with bacterial resistance." Clin Microbiol Rev **12**(4): 501-17.

46. Gillum, A. M., E. Y. Tsay, et al. (1984). "Isolation of the Candida albicans gene for orotidine-5'-phosphate decarboxylase by complementation of S. cerevisiae ura3 and E. coli pyrF mutations." Mol Gen Genet **198**(1): 179-82.

47. Graham, L. A., A. R. Flannery, et al. (2003). "Structure and assembly of the yeast V-ATPase." J Bioenerg Biomembr **35**(4): 301-12.

48. Grant, S. M. a. C., S.P. (1990). "Fluconazole. A review of its pharmacodynamic and pharmacokinetic properties, and therapeutic potential in superficial and systemic mycoses." Drugs **39**: 877-916.

49. Groll, A. H. and T. J. Walsh (2002). "Antifungal chemotherapy: advances and perspectives." Swiss Med Wkly **132**(23-24): 303-11.

50. Grover, D. D., E. Brummer, et al. (1996). "Study of the role of iron in the anticryptococcal activity of human serum and fluconazole." Mycopathologia **133**(2): 71-7.

51. Guillemette, B., A. R. Bataille, et al. (2005). "Variant histone H2A.Z is globally localized to the promoters of inactive yeast genes and regulates nucleosome positioning." PLoS Biol **3**(12): e384.

52. Gupta, A. K. and E. Tomas (2003). "New antifungal agents." Dermatol Clin **21**(3): 565-76.

53. Hanada, T. and A. Yoshimura (2002). "Regulation of cytokine signaling and inflammation." Cytokine Growth Factor Rev **13**(4-5): 413-21.

54. Haynes, K. (2001). "Virulence in Candida species." Trends Microbiol **9**(12): 591-6.

55. Hobson, R. P. (2003). "The global epidemiology of invasive Candida infections--is the tide turning?" J Hosp Infect **55**(3): 159-68; quiz 233.

56. Hubbard, B. K. and C. T. Walsh (2003). "Vancomycin assembly: nature's way." Angew Chem Int Ed Engl **42**(7): 730-65.

57. Jansen, G., C. Wu, et al. (2005). "Drag&Drop cloning in yeast." Gene **344**: 43-51.

58. Jorgensen, P., J. L. Nishikawa, et al. (2002). "Systematic identification of pathways that couple cell growth and division in yeast." Science **297**(5580): 395-400.

59. Kane, P. M. (2006). "The where, when, and how of organelle acidification by the yeast vacuolar H+-ATPase." Microbiol Mol Biol Rev **70**(1): 177-91.

60. Kato, M. and W. Wickner (2001). "Ergosterol is required for the Sec18/ATP-dependent priming step of homotypic vacuole fusion." Embo J **20**(15): 4035-40.

61. Kauffman, C. A. (2006). "Fungal infections." Proc Am Thorac Soc **3**(1): 35-40.

62. Kim, Y. J., L. Francisco, et al. (1994). "Control of cellular morphogenesis by the Ip12/Bem2 GTPase-activating protein: possible role of protein phosphorylation." J Cell Biol **127**(5): 1381-94.

63. Kirkpatrick, C. H. (2001). "Chronic mucocutaneous candidiasis." Pediatr Infect Dis J **20**(2): 197-206.

64. Kontoyiannis, D. P. and R. E. Lewis (2003). "Combination chemotherapy for invasive fungal infections: what laboratory and clinical studies tell us so far." Drug Resist Updat **6**(5): 257-69.

65. Kornberg, R. D. (2005). "Mediator and the mechanism of transcriptional activation." Trends Biochem Sci **30**(5): 235-9.

66. Krogan, N. J., K. Baetz, et al. (2004). "Regulation of chromosome stability by the histone H2A variant Htz1, the Swr1 chromatin remodeling complex, and the histone acetyltransferase NuA4." Proc Natl Acad Sci U S A **101**(37): 13513-8.

67. Larder, B. A., S. D. Kemp, et al. (1995). "Potential mechanism for sustained antiretroviral efficacy of AZT-3TC combination therapy." Science **269**(5224): 696-9

68. Lesage, G., Sdicu, A.-M., MÃ©nard, P., Shapiro, J., Hussein, S. and Bussey, H. (2004). "Analysis of beta-1,3-glucan assembly in Saccharomyces cerevisiae using a synthetic interaction network and altered sensitivity to caspofungin." Genetics **167**: 35-49.

69. Lewis, R. E. and D. P. Kontoyiannis (2001). "Rationale for combination antifungal therapy." Pharmacotherapy **21**(8 Pt 2): 149S-164S.

70. MacPherson, S., B. Akache, et al. (2005). "Candida albicans zinc cluster protein Upc2p confers resistance to antifungal drugs and is an activator of ergosterol biosynthetic genes." Antimicrob Agents Chemother **49**(5): 1745-52.

71. Marr, K. A. (2004). "Invasive Candida infections: the changing epidemiology." Oncology (Williston Park) **18**(14 Suppl 13): 9-14.

72. Mazzoni, C., P. Zarov, et al. (1993). "The SLT2 (MPK1) MAP kinase homolog is involved in polarized cell growth in Saccharomyces cerevisiae." J Cell Biol **123**(6 Pt 2): 1821-33.

73. Milgrom, E., R. W. West, Jr., et al. (2005). "TFIID and Spt-Ada-Gcn5-acetyltransferase functions probed by genome-wide synthetic genetic array analysis using a Saccharomyces cerevisiae taf9-ts allele." Genetics **171**(3): 959-73.

74. Milgrom, E., H. Diab, et al. (2007). "Loss of vacuolar proton-translocating ATPase activity in yeast results in chronic oxidative stress." J Biol Chem **282**(10): 7125-36.

75. Moellering, R. C., P. K. Linden, et al. (1999). "The efficacy and safety of quinupristin/dalfopristin for the treatment of infections caused by vancomycin-resistant Enterococcus faecium. Synercid Emergency-Use Study Group." J Antimicrob Chemother **44**(2): 251-61.

76. Morris, M. I. and M. Villmann (2006). "Echinocandins in the management of invasive fungal infections, Part 2." Am J Health Syst Pharm **63**(19): 1813-20.

77. Morschhauser, J., K. S. Barker, et al. (2007). "The transcription factor Mrr1p controls expression of the MDR1 efflux pump and mediates multidrug resistance in Candida albicans." PLoS Pathog **3**(11): e164.

78. Naglik, J. R., S. J. Challacombe, et al. (2003). "Candida albicans secreted aspartyl proteinases in virulence and pathogenesis." Microbiol Mol Biol Rev **67**(3): 400-28, table of contents.

79. Oluwatosin, Y. E. and P.M. Kane (1998)."Mutations in the yeast KEX2 gene cause a Vma(-)-like phenotype: a possible role for the Kex2 endoprotease in vacuolar acidification." Mol Cell Biol **18**(3): 1534-43.

80. Onyewu, C., Blankenship, J.R., Del Poeta, M. and Heitman, J. (2003). "Ergosterol biosynthesis inhibitors become fungicidal when combined with calcineurin inhibitors against Candida albicans, Candida glabrata, and Candida krusei." Antimicrob Agents Chemother **47**: 956-96.

81. Onyewu, C., N. A. Afshari, et al. (2006). "Calcineurin promotes infection of the cornea by Candida albicans and can be targeted to enhance fluconazole therapy." Antimicrob Agents Chemother **50**(11): 3963-5.

82. Perea, S., J. L. Lopez-Ribot, et al. (2001). "Prevalence of molecular mechanisms of resistance to azole antifungal agents in Candida albicans strains displaying high-level

fluconazole resistance isolated from human immunodeficiency virus-infected patients." Antimicrob Agents Chemother **45**(10): 2676-84.

83. Perlin, D. S. (2007). "Resistance to echinocandin-class antifungal drugs." Drug Resist Updat **10**(3): 121-30.

84. Peterson, J., Y. Zheng, et al. (1994). "Interactions between the bud emergence proteins Bem1p and Bem2p and Rho-type GTPases in yeast." J Cell Biol **127**(5): 1395-406.

85. Poon, P. P., X. Wang, et al. (1996). "Saccharomyces cerevisiae Gcs1 is an ADP-ribosylation factor GTPase-activating protein." Proc Natl Acad Sci U S A **93**(19): 10074-7.

86. Razzaque, M. S., M. A. Hossain, et al. (2001). "Lipid formulations of polyene antifungal drugs and attenuation of associated nephrotoxicity." Nephron **89**(3): 251-4.

87. Ribeiro, M. A. and C. R. Paula (2007). "Up-regulation of ERG11 gene among fluconazole-resistant Candida albicans generated in vitro: is there any clinical implication?" Diagn Microbiol Infect Dis **57**(1): 71-5.

88. Roberts, S. M. and F. Winston (1996). "SPT20/ADA5 encodes a novel protein functionally related to the TATA-binding protein and important for transcription in Saccharomyces cerevisiae." Mol Cell Biol **16**(6): 3206-13.

89. Rooney, P. J. and B. S. Klein (2002). "Linking fungal morphogenesis with virulence." Cell Microbiol **4**(3): 127-37.

90. Saleh, A., V. Lang, et al. (1997). "Identification of native complexes containing the yeast coactivator/repressor proteins NGG1/ADA3 and ADA2." J Biol Chem **272**(9): 5571-8.

91. Sambade, M., M. Alba, et al. (2005). "A genomic screen for yeast vacuolar membrane ATPase mutants." Genetics **170**(4): 1539-51.

92. Sanglard, D., K. Kuchler, et al. (1995). "Mechanisms of resistance to azole antifungal agents in Candida albicans isolates from AIDS patients involve specific multidrug transporters." Antimicrob Agents Chemother **39**(11): 2378-86.

93. Sanglard, D. and F. C. Odds (2002). "Resistance of Candida species to antifungal agents: molecular mechanisms and clinical consequences." Lancet Infect Dis **2**(2): 73-85.

94. Schoondermark-Stolk, S.A., Jansen, M.A., et al. (2006). “Genome-wide transcription survey on flavour production in Saccharomyces cerevisiae.” World J Microbiol Biotechnol **22**:1347–1356

95. Schuldiner, M., Collins, S.R., Thompson, N.J., Denic, V., Bhamidipati, A., Punna, T., Ihmels, J., Andrews, B., Boone, C., Greenblatt, J.F. et al. (2005). "Exploration of the function and organization of the yeast early secretory pathway through an epistatic miniarray profile." Cell **123**: 507--519.

96. Song, W., I. Treich, et al. (1996). "SSN genes that affect transcriptional repression in Saccharomyces cerevisiae encode SIN4, ROX3, and SRB proteins associated with RNA polymerase II." Mol Cell Biol **16**(1): 115-20.

97. Stark, C., B. J. Breitkreutz, et al. (2006). "BioGRID: a general repository for interaction datasets." Nucleic Acids Res **34**(Database issue): D535-9.

98. Stoj, C. S., A. J. Augustine, et al. (2006). "Structural basis of the ferrous iron specificity of the yeast ferroxidase, Fet3p." Biochemistry **45**(42): 12741-9.

99. Tatebayashi, K., K. Yamamoto, et al. (2006). "Adaptor functions of Cdc42, Ste50, and Sho1 in the yeast osmoregulatory HOG MAPK pathway." Embo J **25**(13): 3033-44.

100. Umebayashi, K. and A. Nakano (2003). "Ergosterol is required for targeting of tryptophan permease to the yeast plasma membrane." J Cell Biol **161**(6): 1117-31.

101. Usaite, R., K. R. Patil, et al. (2006). "Global transcriptional and physiological responses of Saccharomyces cerevisiae to ammonium, L-alanine, or L-glutamine limitation." Appl Environ Microbiol **72**(9): 6194-203.

102. van Voorst, F., Houghton-Larsen, J., Jønson, L., Kielland-Brandt, M.C. and Brandt, A. (2006). "Genome-wide identification of genes required for growth of Saccharomyces cerevisiae under ethanol stress." Yeast **23**: 351-359.

103. Verduyn Lunel, F. M., J. F. Meis, et al. (1999). "Nosocomial fungal infections: candidemia." Diagn Microbiol Infect Dis **34**(3): 213-20.

104. Vincent, J. L., E. Anaissie, et al. (1998). "Epidemiology, diagnosis and treatment of systemic Candida infection in surgical patients under intensive care." Intensive Care Med **24**(3): 206-16.

105. Wagner, C., W. Graninger, et al. (2006). "The echinocandins: comparison of their pharmacokinetics, pharmacodynamics and clinical applications." Pharmacology **78**(4): 161-77.

106. Wang, T. and A. Bretscher (1995). "The rho-GAP encoded by BEM2 regulates cytoskeletal structure in budding yeast." Mol Biol Cell **6**(8): 1011-24.

107. Ward, J. H. (1963). “Hierarchical grouping to optimise an objective function.” Journal of the American Statistical Association **58**: 236-244.

108. White, T. C., K. A. Marr, et al. (1998). "Clinical, cellular, and molecular factors that contribute to antifungal drug resistance." Clin Microbiol Rev **11**(2): 382-402.

109. Wu, W. H., S. Alami, et al. (2005). "Swc2 is a widely conserved H2AZ-binding module essential for ATP-dependent histone exchange." Nat Struct Mol Biol **12**(12): 1064-71.

110. Yoshida, Y. and Y. Aoyama (1987). "Interaction of azole antifungal agents with cytochrome P-45014DM purified from Saccharomyces cerevisiae microsomes." Biochem Pharmacol **36**(2): 229-35.

111. Zhang, J. W., K. J. Parra, et al. (1998). "Characterization of a temperature-sensitive yeast vacuolar ATPase mutant with defects in actin distribution and bud morphology." J Biol Chem **273**(29): 18470-80.